Electronic Supplementary Material (ESI) for RSC Advances.

Tuning Anticancer Properties and DNA-binding of Pt(II) Complexes via Alteration of Nitrogen Softness/Basicity of Tridentate Ligands

Kamelah S. Al-Rashdi [a,b], Bandar A. Babgi [a *], Ehab M. M. Ali [c,d], Abdesslem Jedidi [a], Abdul-Hamid M. Emwas [e], Bambar Davaasuren [e],Mariusz Jaremko [f], Mark G. Humphrey [g]

[a] Department of Chemistry, Faculty of Science, King Abdulaziz University, P.O. Box 80203, Jeddah 21589, Saudi Arabia.

[b] Department of Chemistry, Faculty of Science, Umm Al-qura University, Al-Qunfudah University College, Al-Qunfudah 21912, Saudi Arabia.

[c] Department of Biochemistry, Faculty of Science, King Abdulaziz University, P.O. Box 80203, Jeddah 21589, Saudi Arabia.

[d] Division of Biochemistry, Department of Chemistry, Faculty of Science, Tanta University, Tanta 31527, Egypt

[e] Core Labs, King Abdullah University of Science and Technology (KAUST), Thuwal, 23955-6900, Saudi Arabia.

[f] King Abdullah University of Science and Technology (KAUST), Biological and Environmental Science and Engineering (BESE), Thuwal, 23955-6900, Saudi Arabia.

[g] Research School of Chemistry, Australian National University, Canberra, ACT 2601, Australia.* Correspondence author. Ph: +966 555563702; email: bbabgi@kau.edu.sa.

NMR

Ligand 1 (L-PhN-OEt)

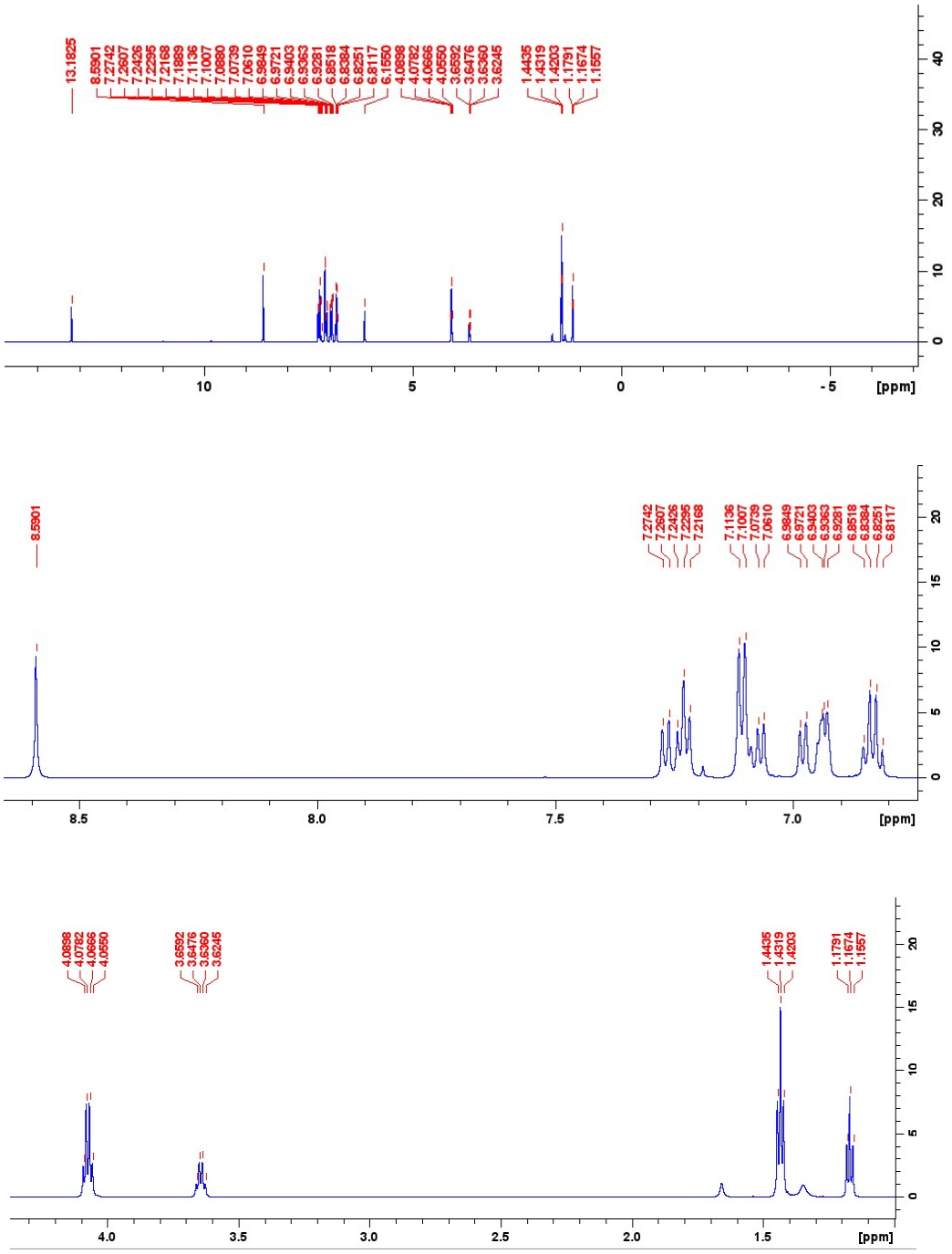

Figure S1. ^{1}H NMR of ligand 1 (L-PhN-OEt).

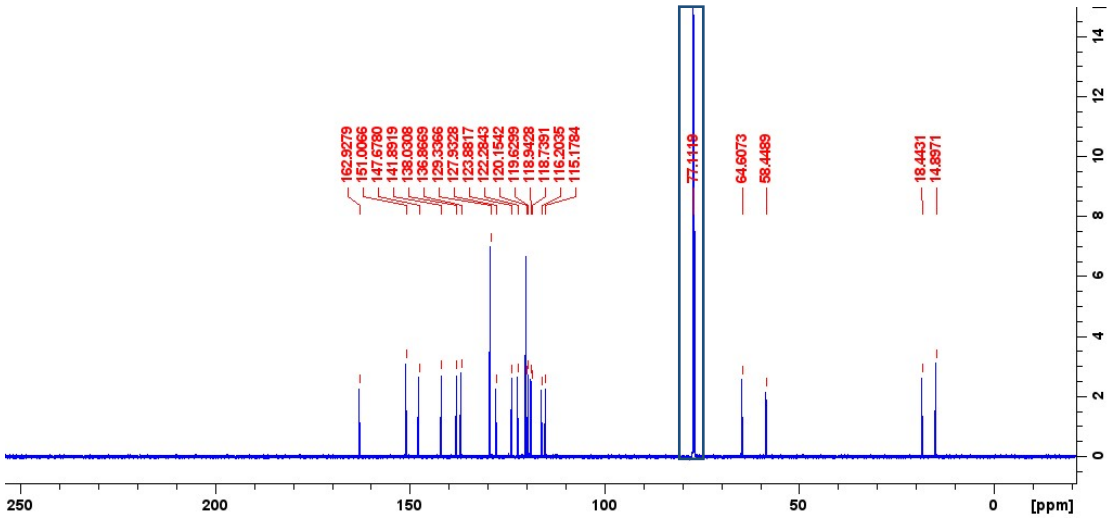

Figure S2. ^{13}C NMR of of ligand 1 (L-PhN-OEt).

Ligand 2 (L-PhN-NEt_2)

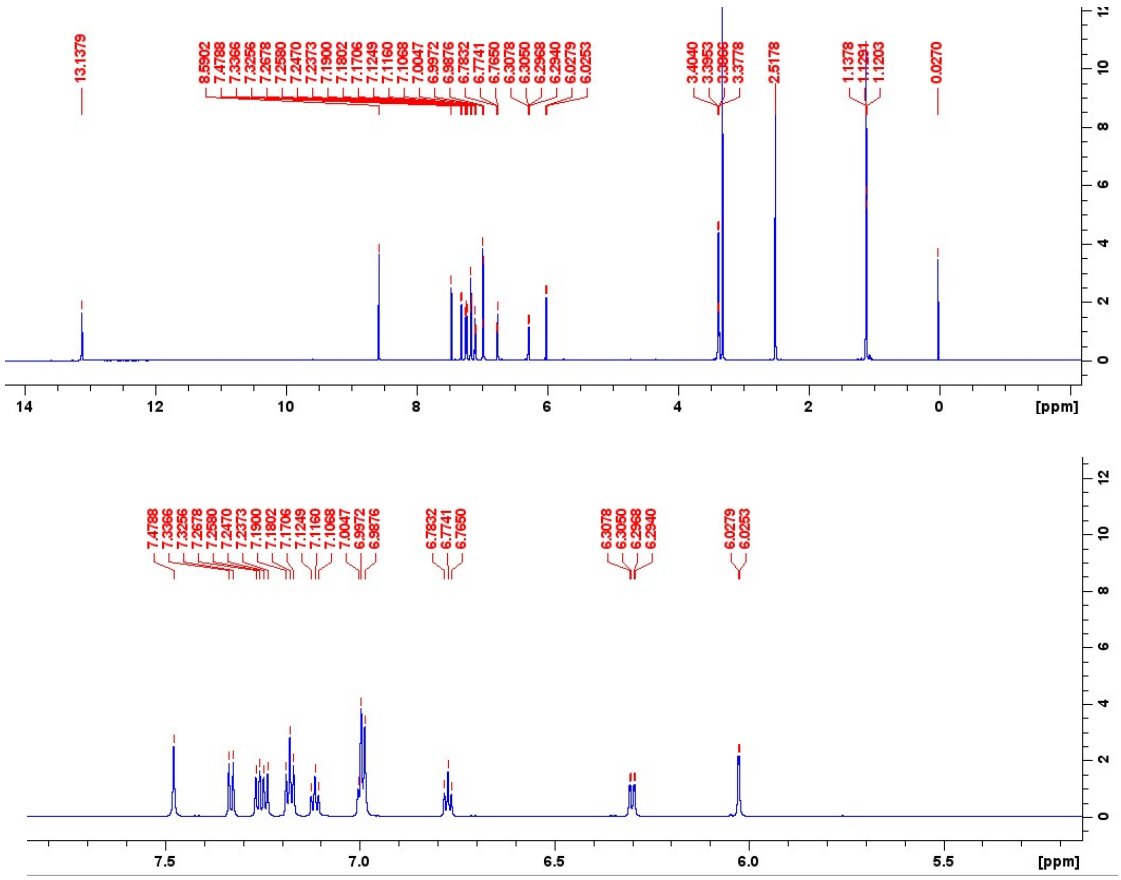

Figure S3. ^{1}H NMR of ligand 2 (L-PhN-NEt_2).

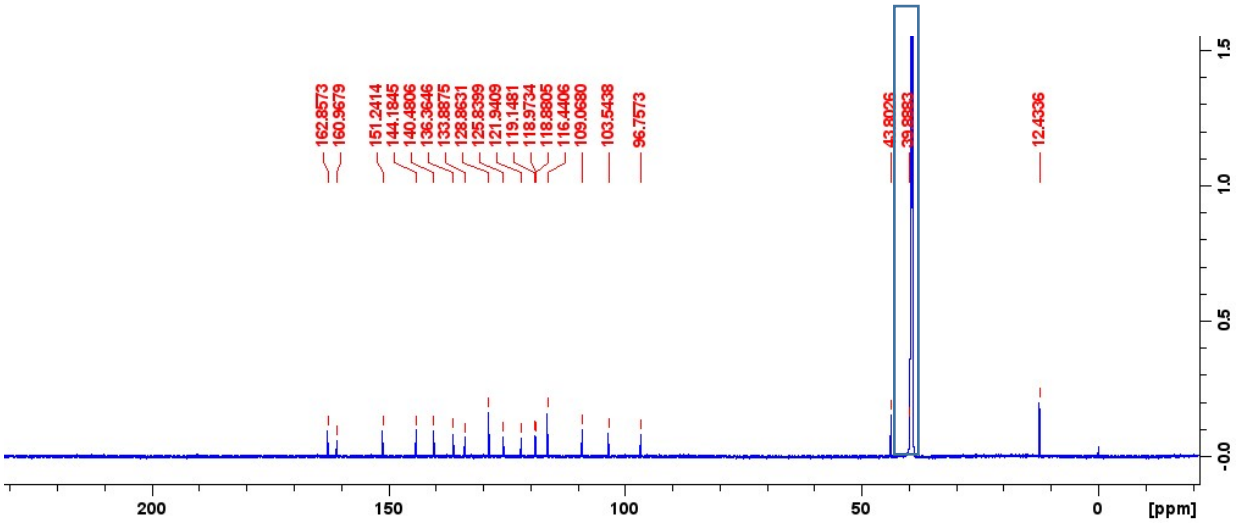

Figure S4. ^{13}C NMR of ligand 2 (L-PhN-NEt_2).

Ligand 3 (L-PhN-OH)

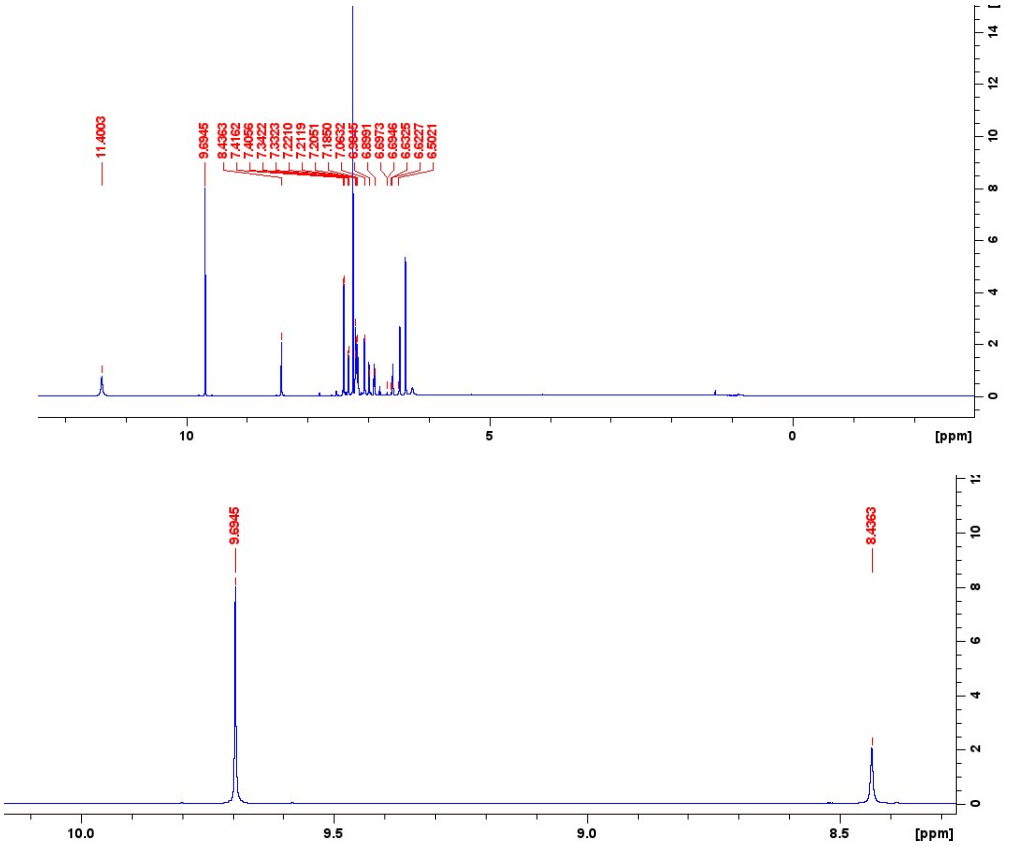

Figure S5. ^{1}H NMR of ligand 3 (L-PhN-OH).

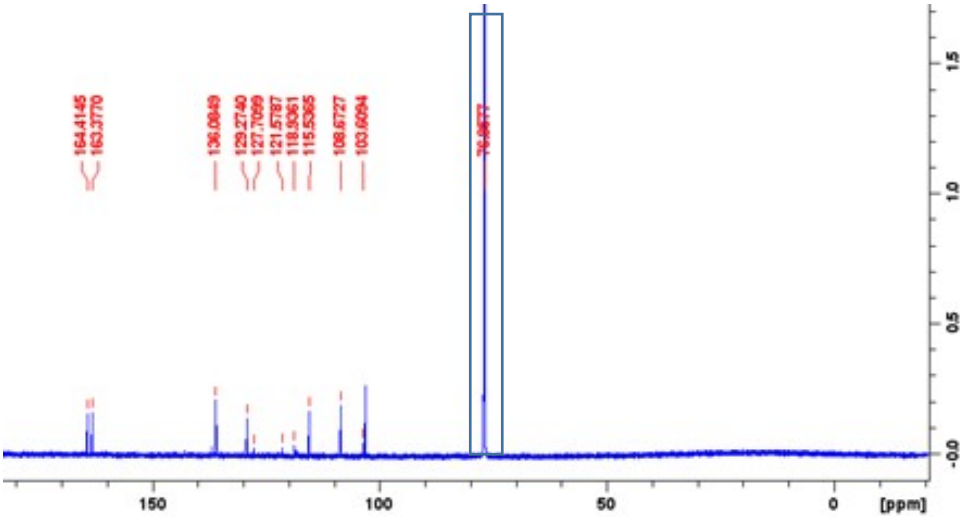

Figure S6. ^{13}C NMR of ligand 3 (L-PhN-OH).

Ligand 4 (L-EN-OEt)

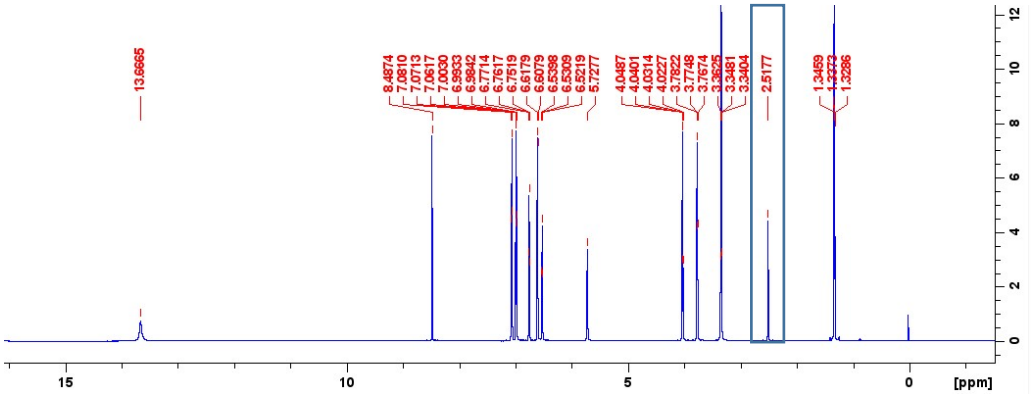

Figure S7. ^{1}H NMR of ligand 4 (L-EN-OEt).

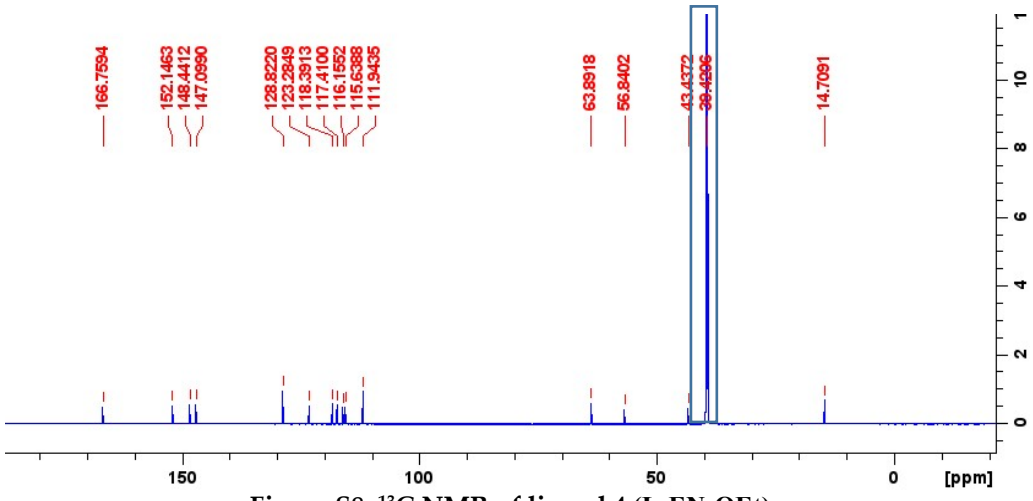

Figure S8. ^{13}C NMR of ligand 4 (L-EN-OEt).

Ligand 5 (L-EN-NEt$_2$)

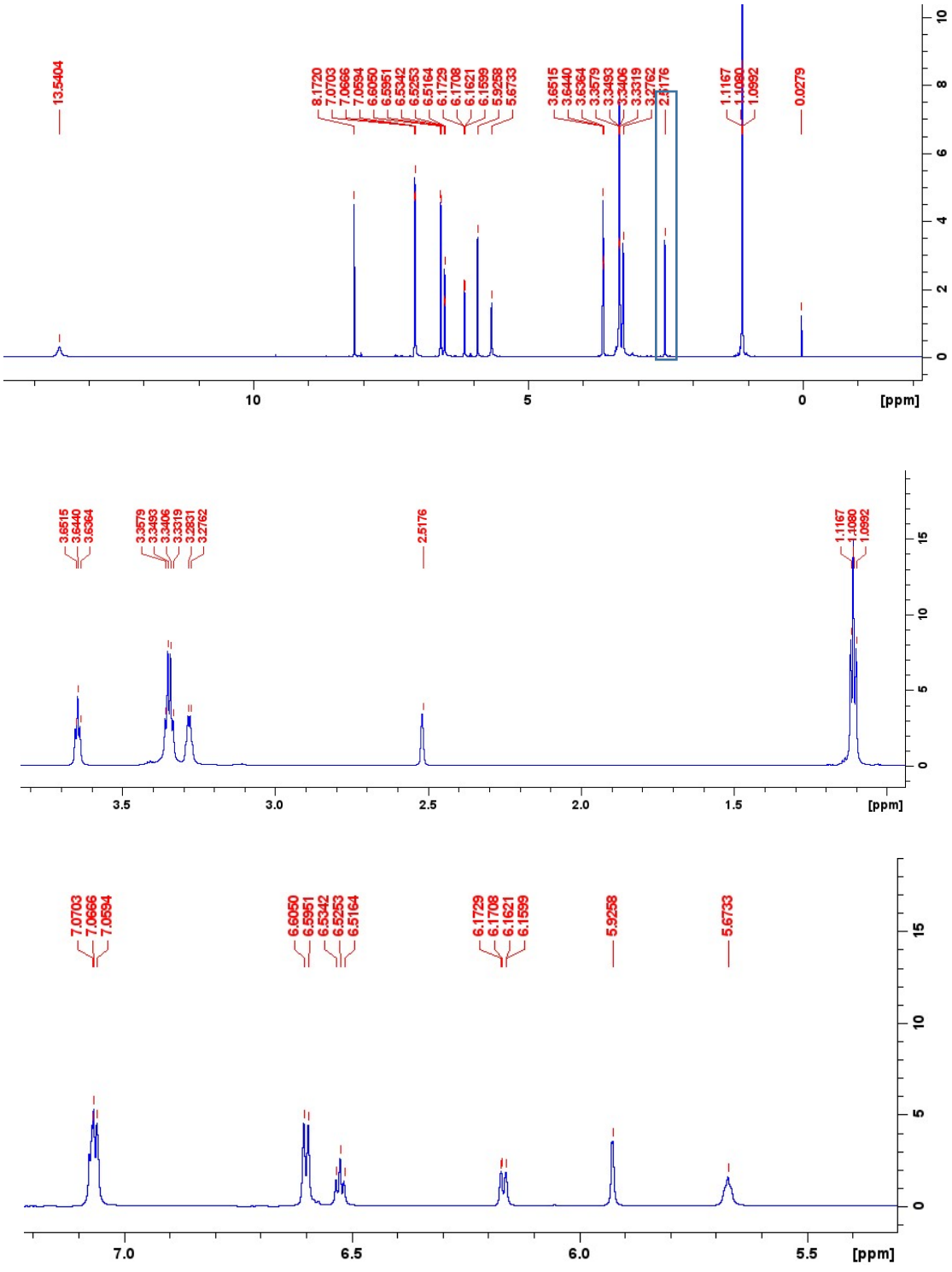

Figure S9. ^{1}H NMR of ligand 5 (L-EN-NEt$_2$).

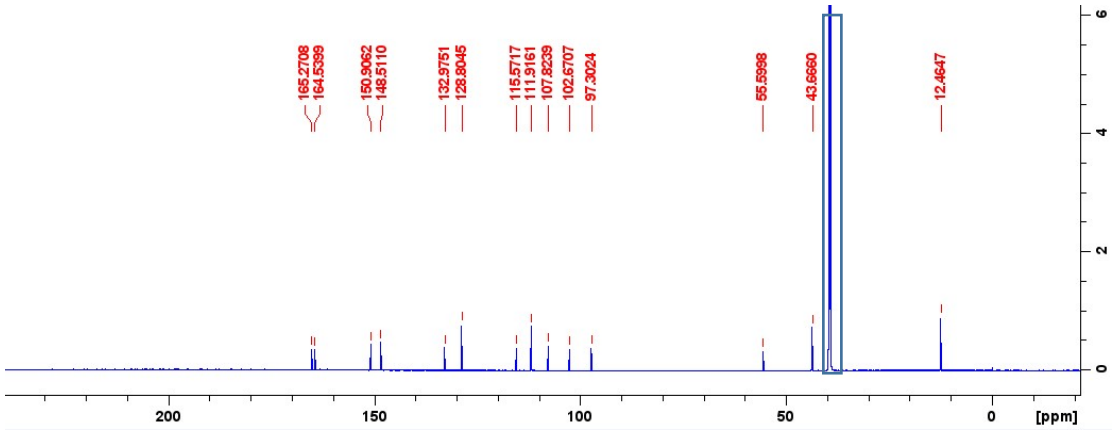

Figure S10. ^{13}C NMR of ligand 5 (L-EN-NEt_2).

Ligand 6 (L-EN-OH)

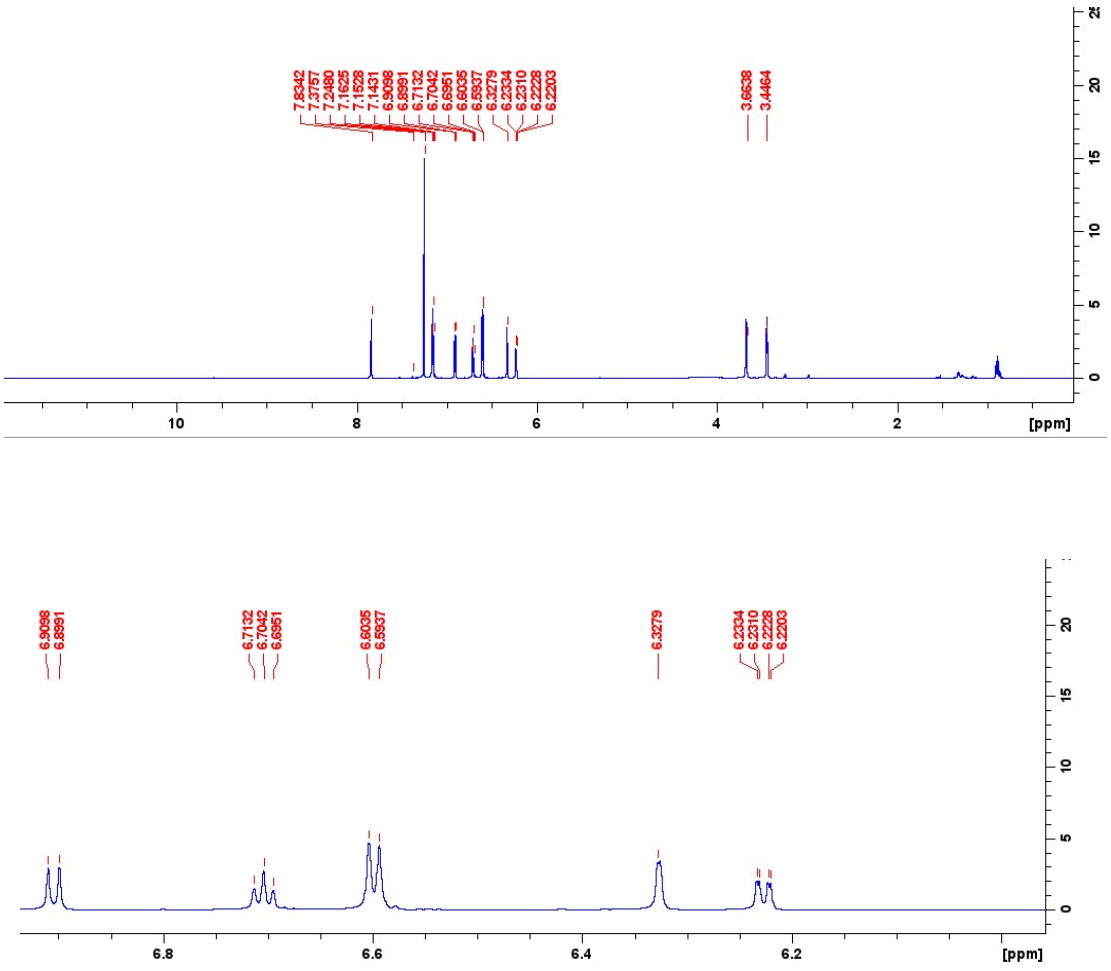

Figure S11. ^{1}H NMR of ligand 6 (L-EN-OH).

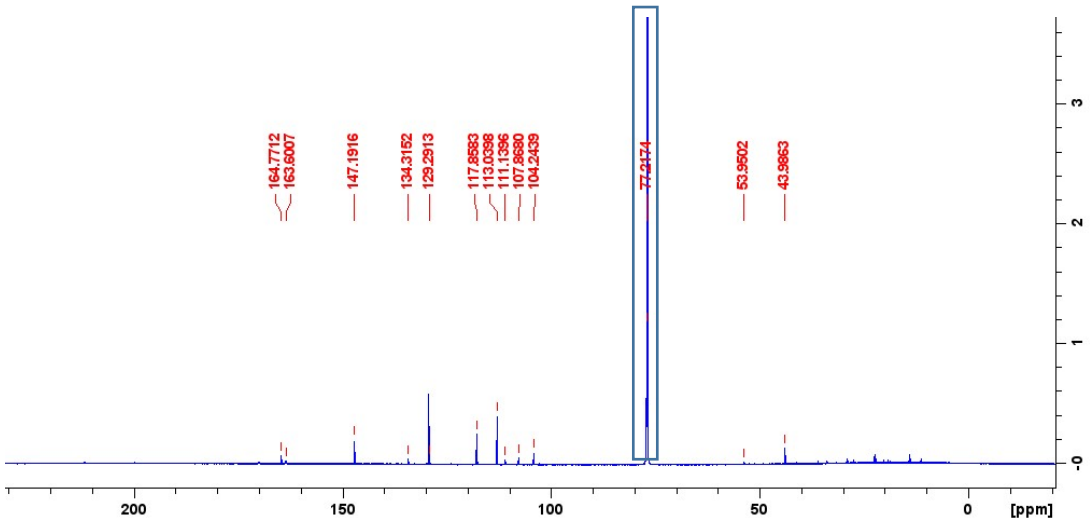

Figure S12. ^{13}C NMR of ligand 6 (L-EN-OH).

Pt-PhN-OEt

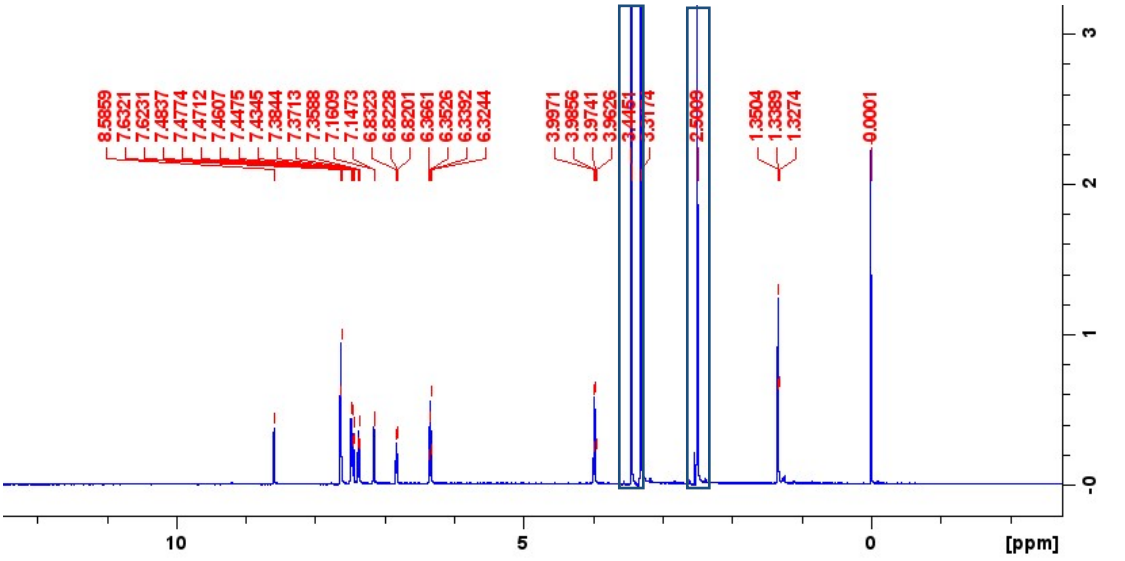

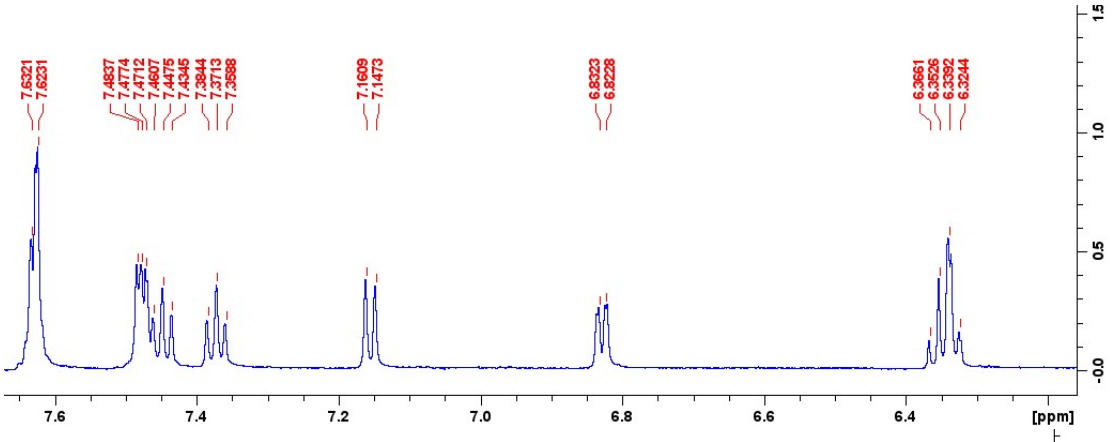

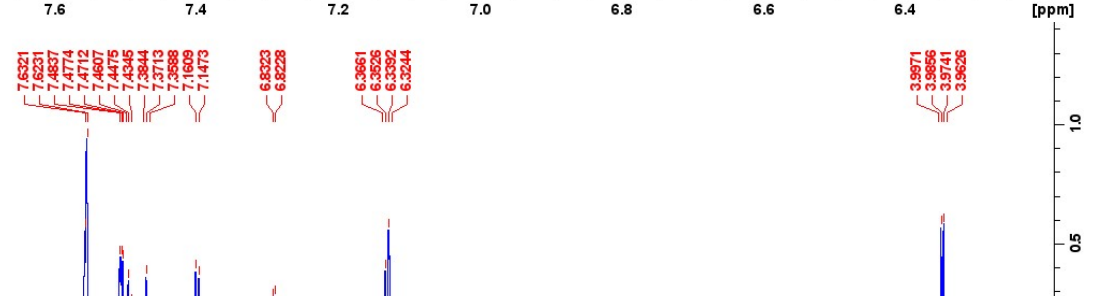

Figure S13. ^{1}H NMR of Pt-PhN-OEt.

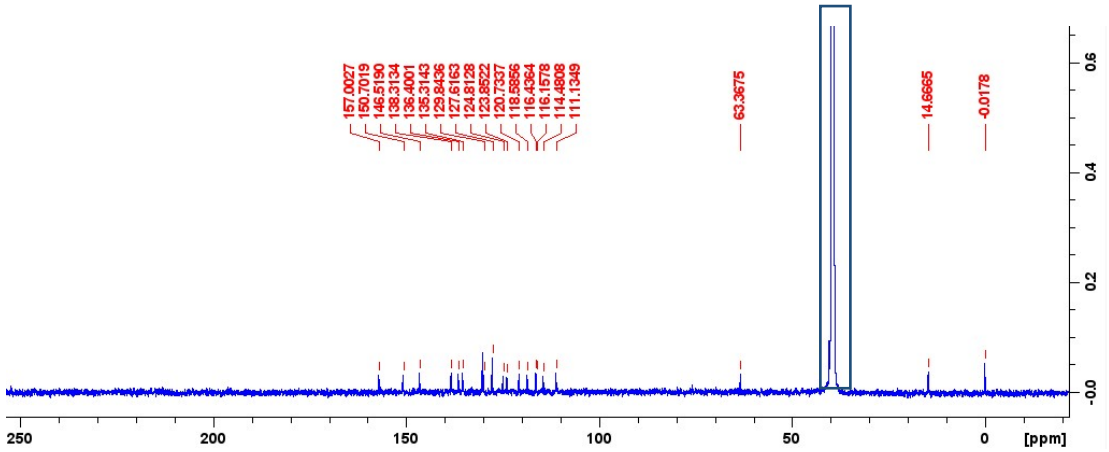

Figure S14. ^{13}C NMR of complex of Pt-PhN-OEt.

Pt-PhN-NEt_2

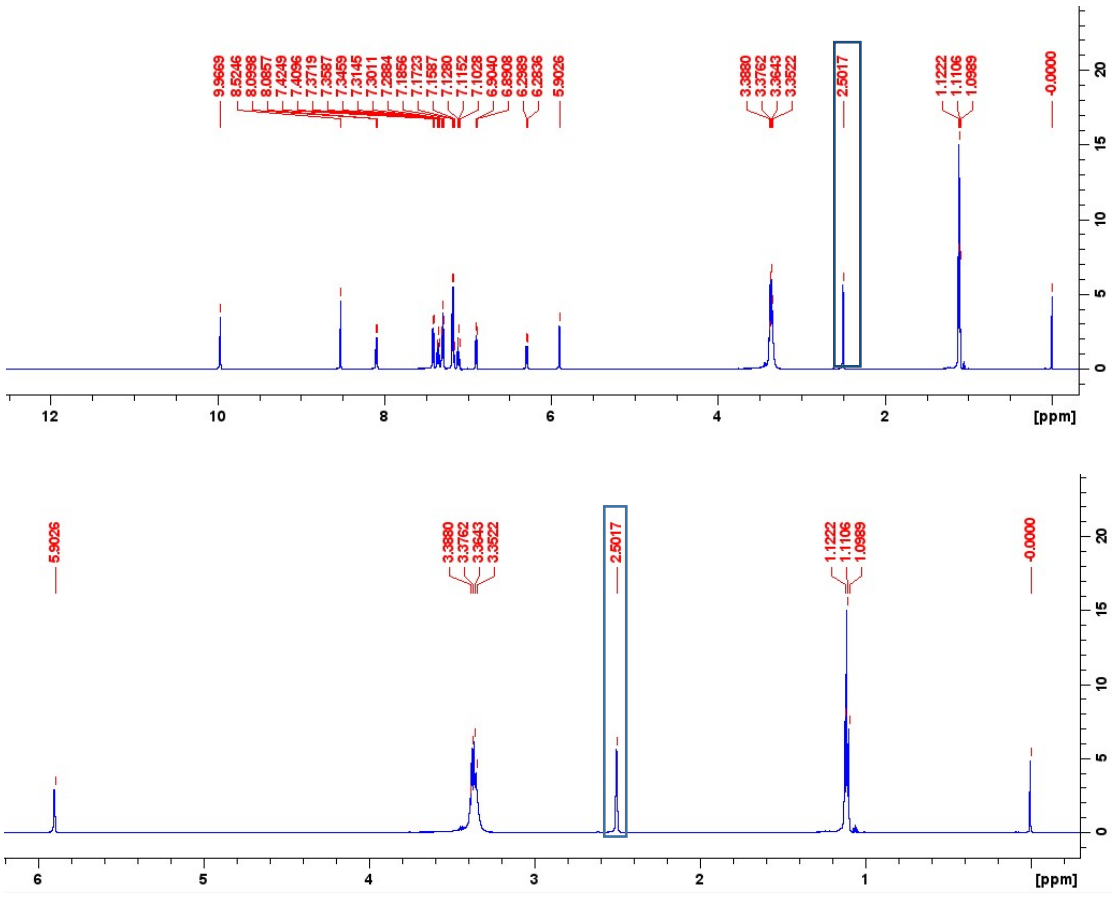

Figure S15. ^{1}H NMR of complex Pt-PhN-NEt_2.

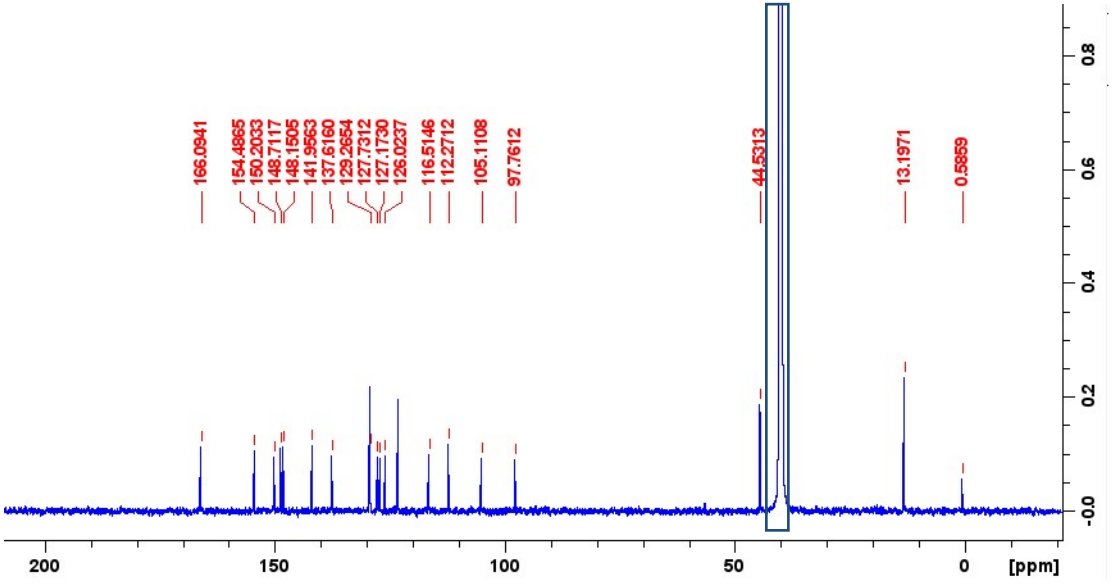

Figure S16. ^{13}C NMR of complex Pt-PhN-NEt_2.

Pt-PhN-OH

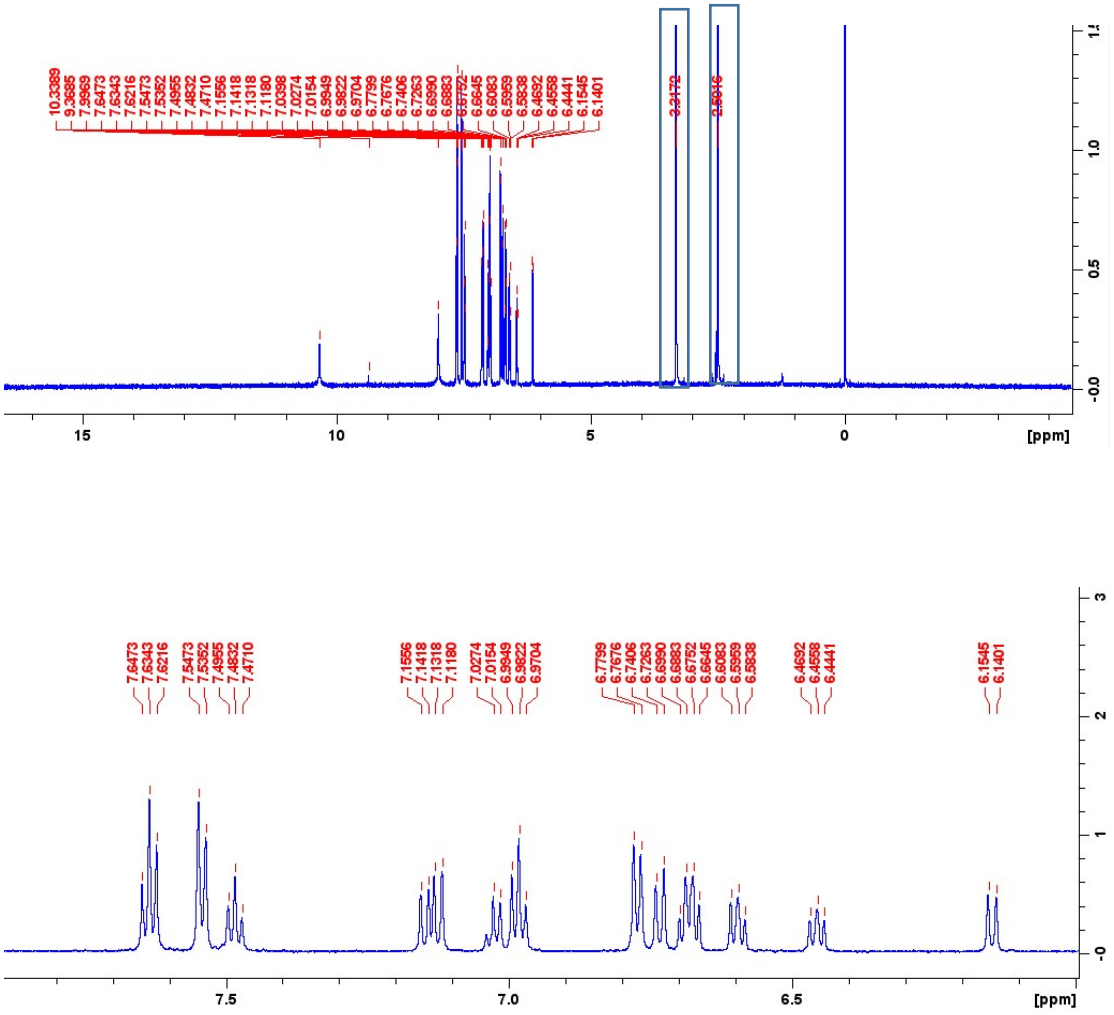

Figure S17. ^{1}H NMR of complex Pt-PhN-OH.

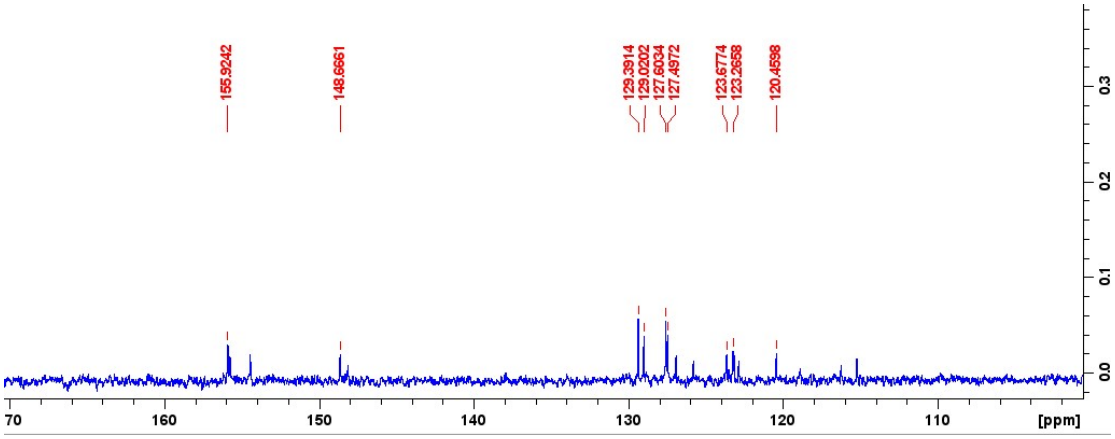

Figure S18. ^{13}C NMR of complex Pt-PhN-OH.

Pt-EN-OEt

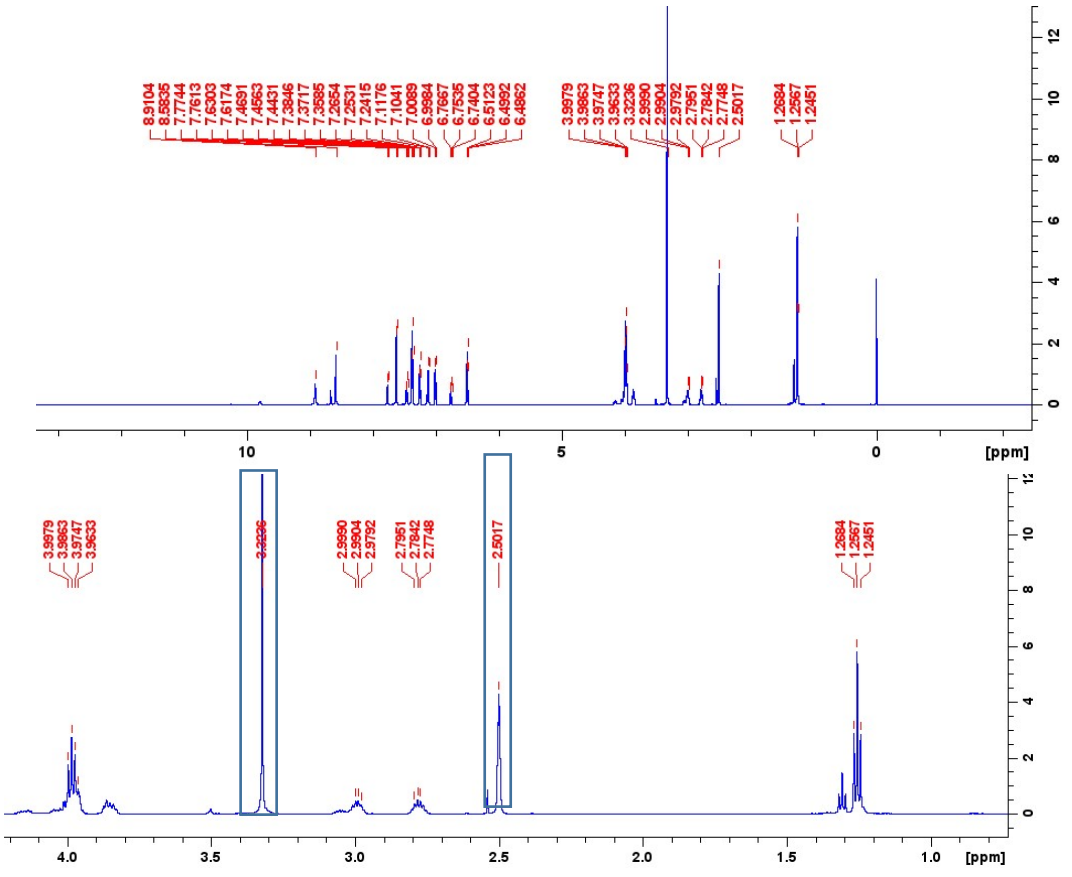

Figure S19. ^{1}H NMR of complex Pt-EN-OEt.

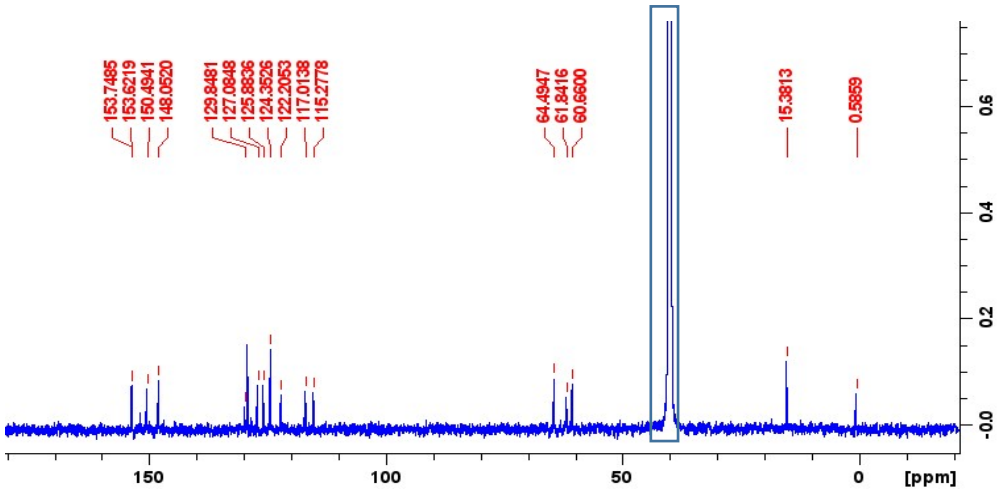

Figure S20. ^{13}C NMR of complex Pt-EN-OEt.

Pt-EN-NEt_2

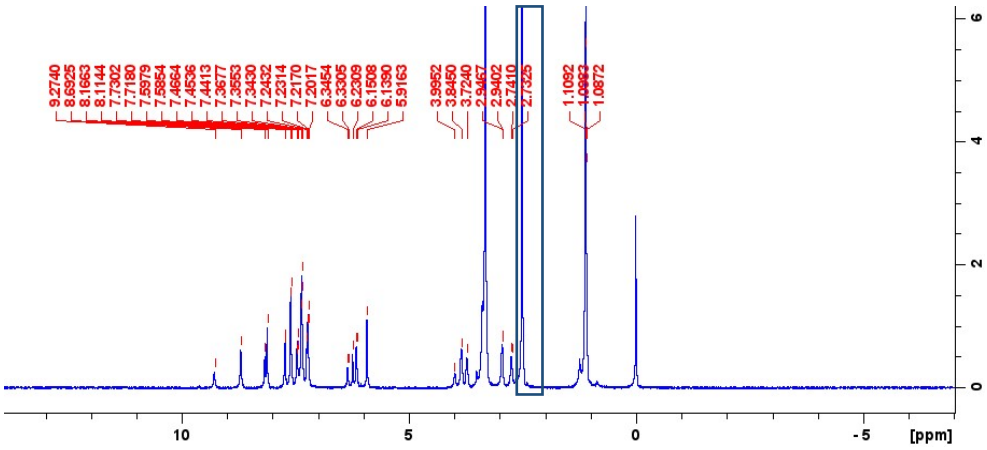

Figure S21. ^{1}H NMR of complex Pt-EN-NEt_2.

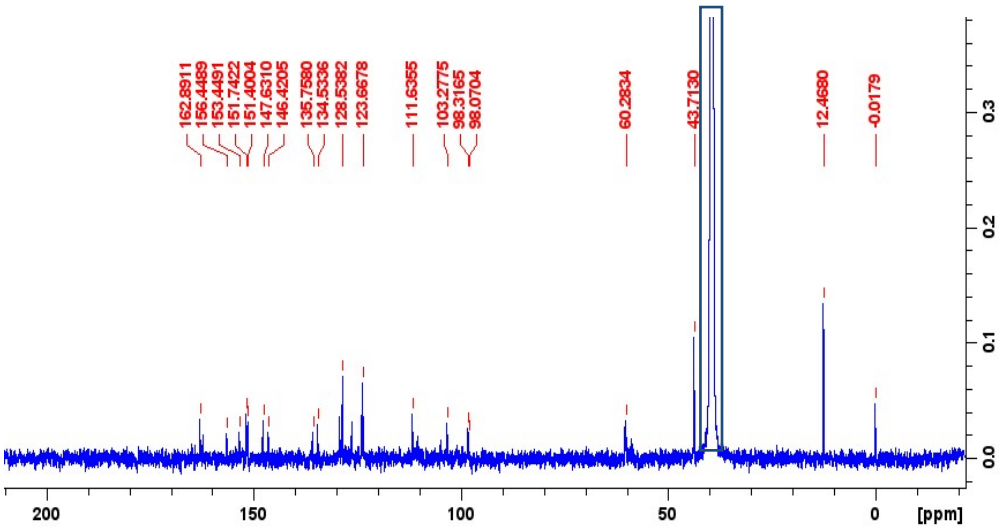

Figure S22. ^{13}C NMR of complex Pt-EN-NEt_2.

Pt-EN-OH

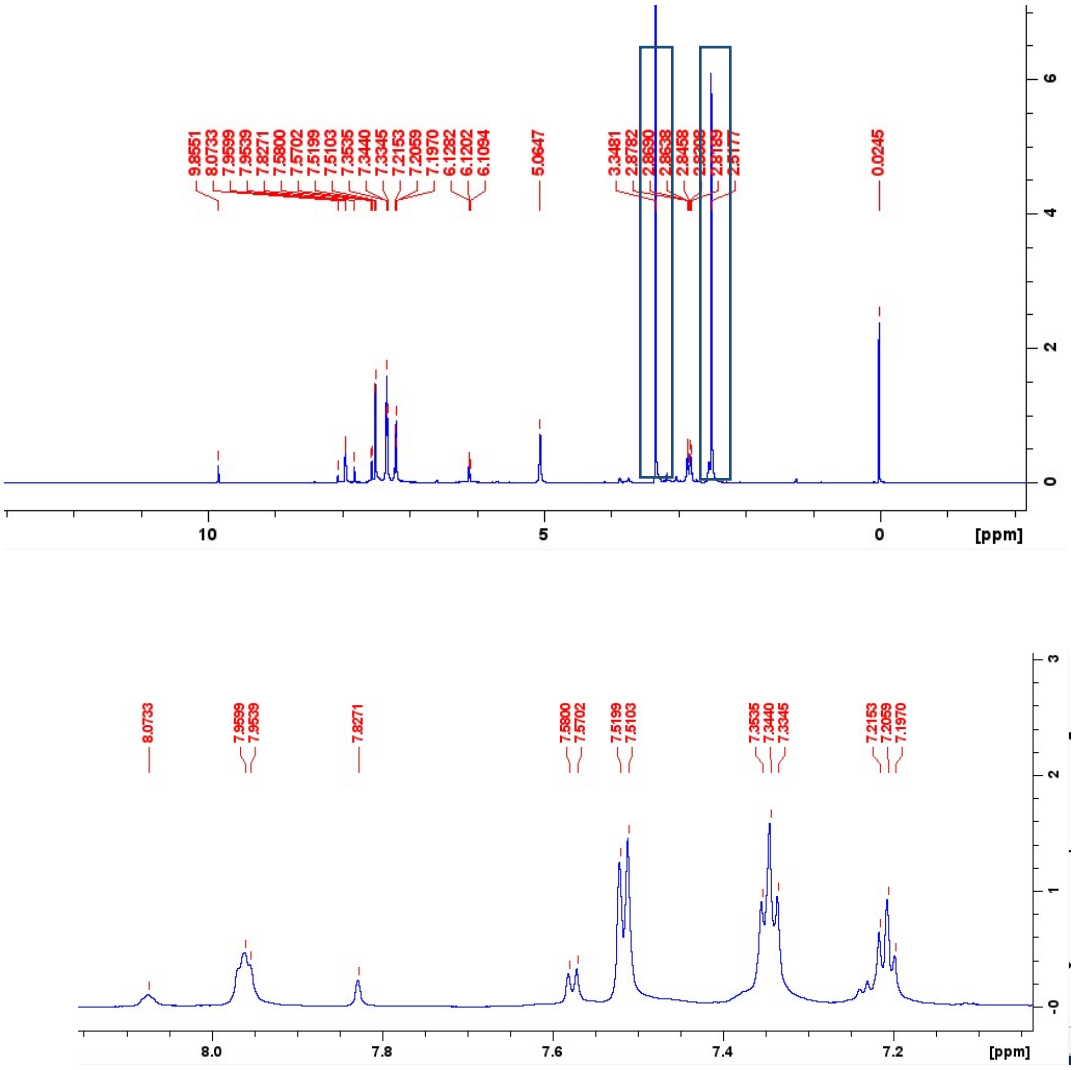

Figure S23. ^{1}H NMR of Complex Pt-EN-OH.

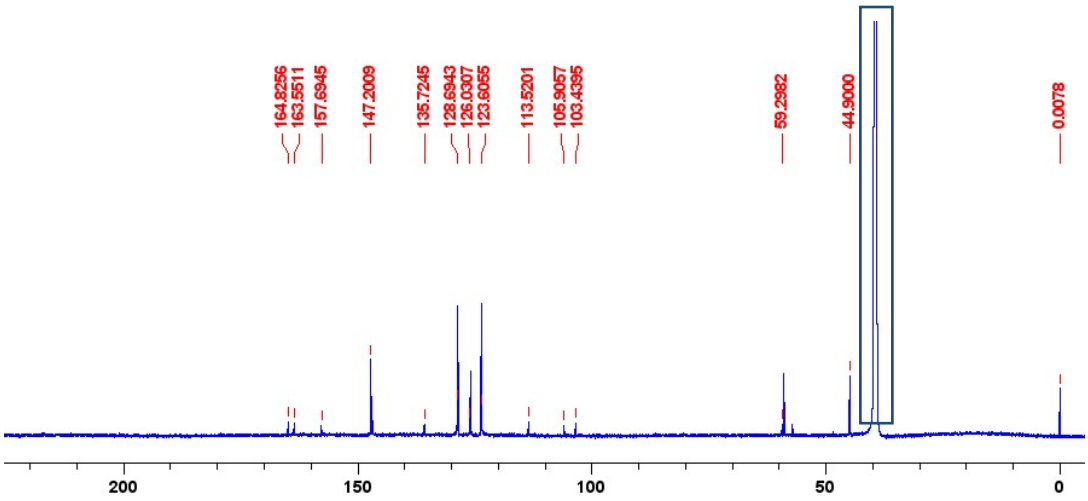

Figure S24. ^{13}C NMR of Complex Pt-EN-OH.

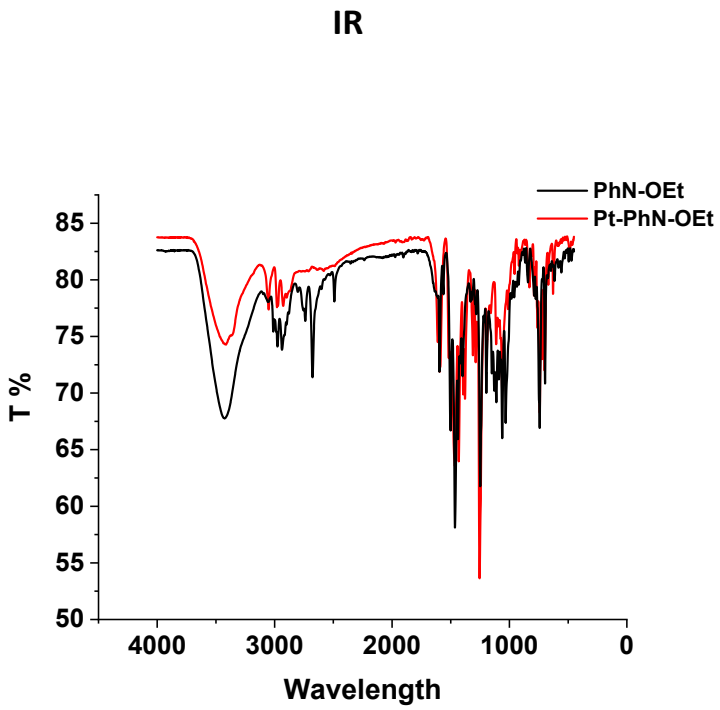

Figure S25. IR of Complex Pt- PhN-OEt.

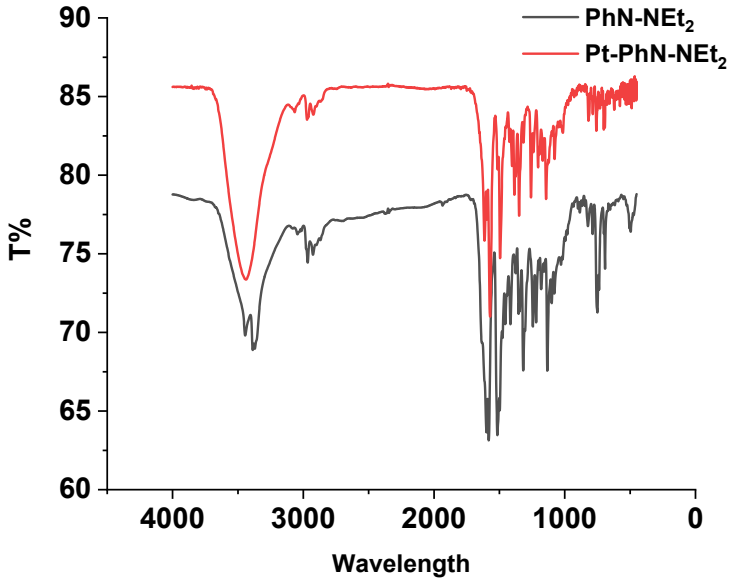

Figure S26. IR of Complex Pt- PhN-NEt_2.

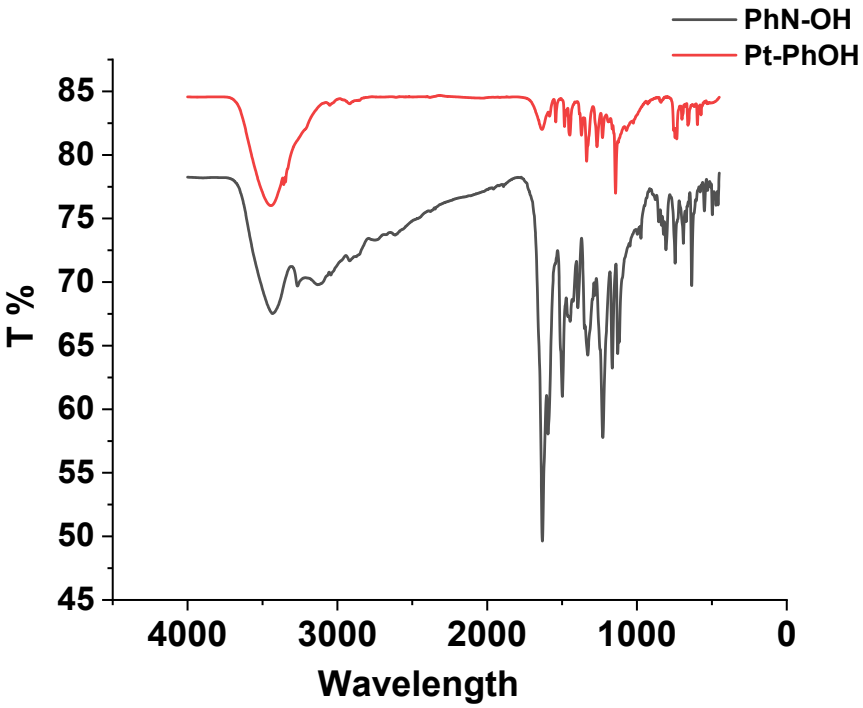

Figure S27. IR of Complex Pt- PhN-OH.

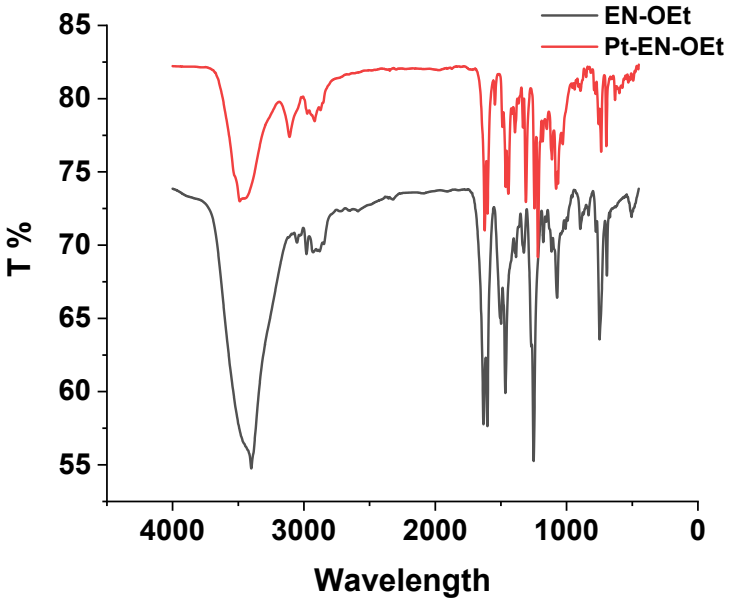

Figure S28. IR of Complex Pt- EN-OEt.

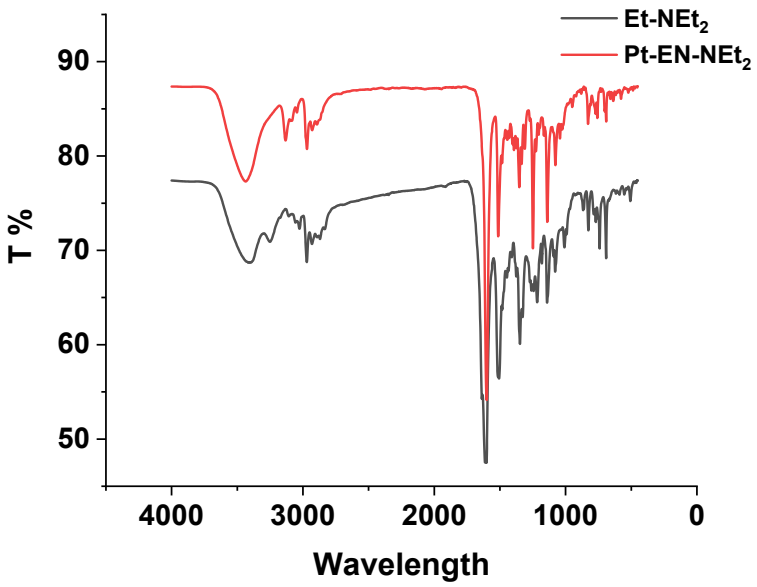

Figure S29. IR of Complex Pt- EN-NEt_2

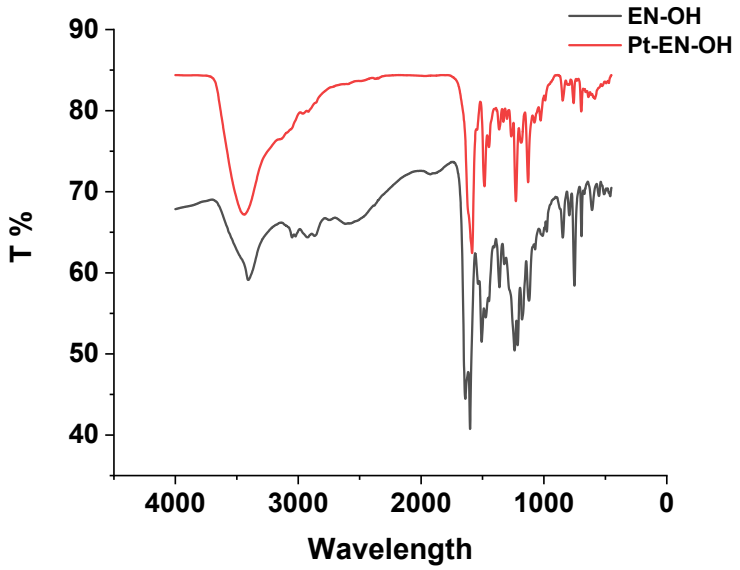

Figure S30. IR of Complex Pt- EN-OH.

Crystallographic of L5(L-EN-NEt_2)

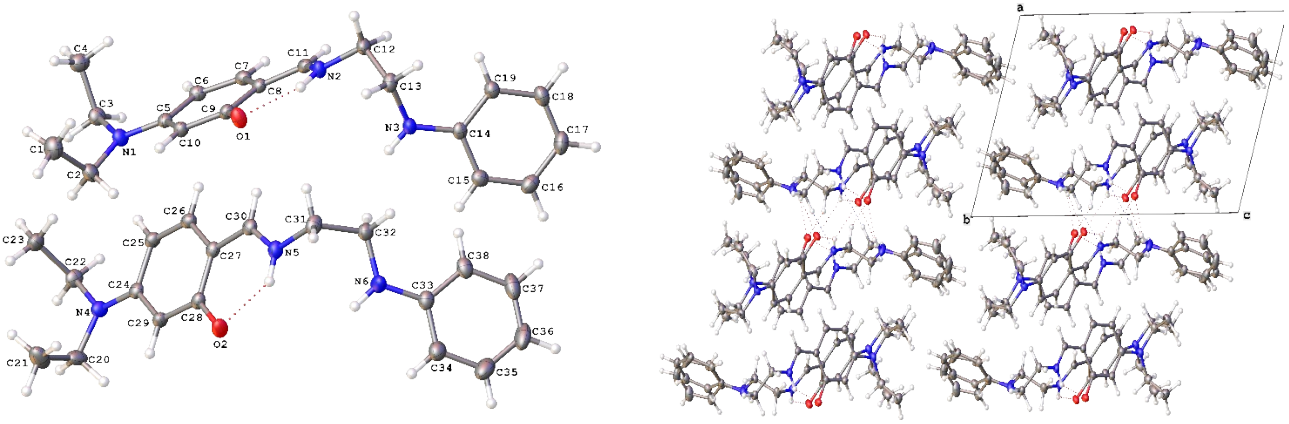

Figure S31. Crystal structure of L5(L-EN-NEt_2).

DNA-Binding Studies

Competitive Fluorescence Quenching of Ethidium Bromide-DNA Adduct

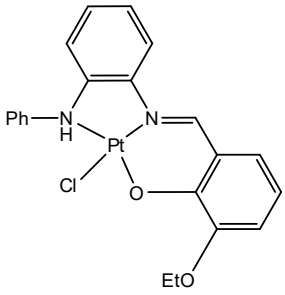

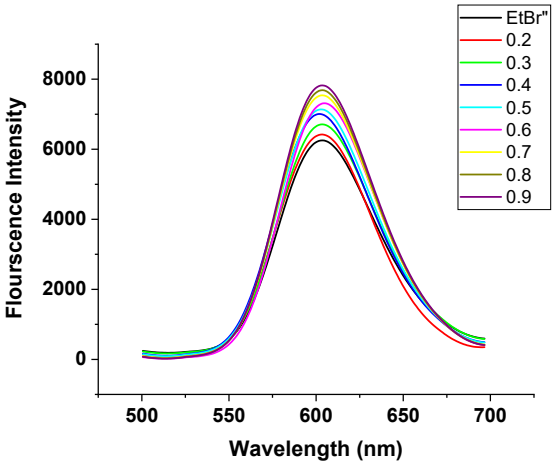

Figure S32. Assessment of DNA binding affinities of Pt-PhN-OEt by fluorescence competitive quenching of EB-DNA adduct.

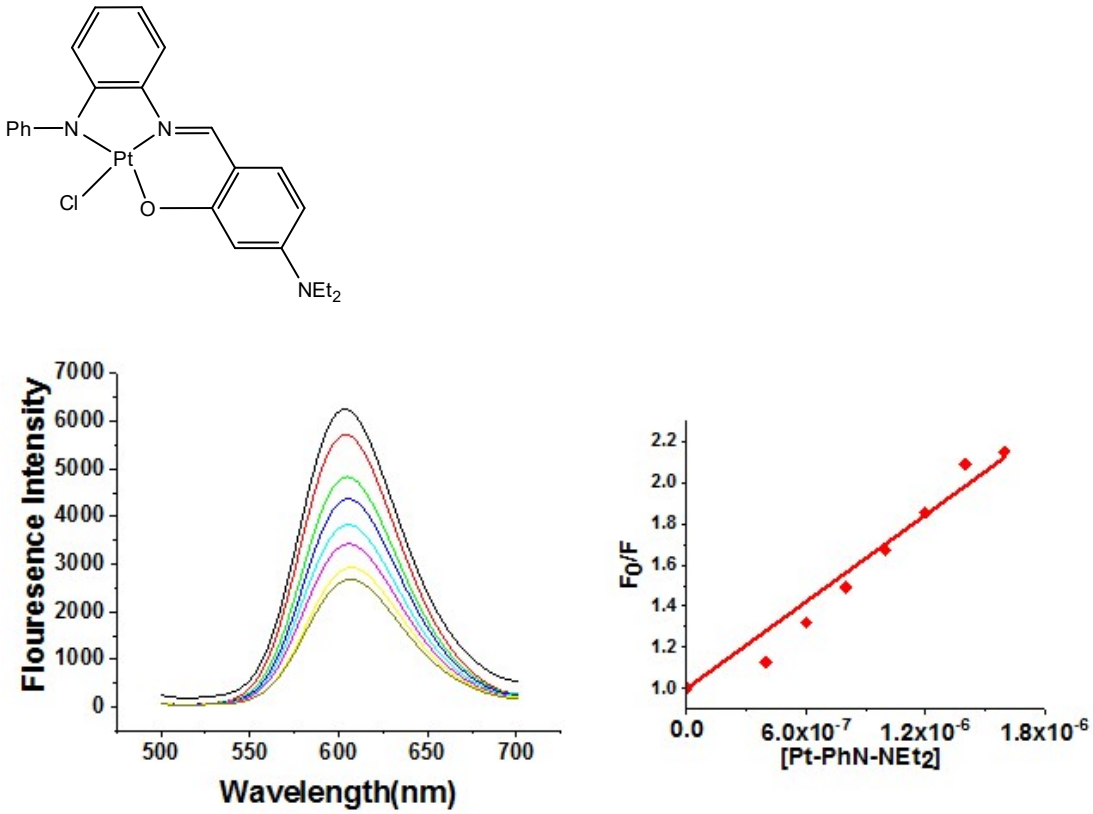

Figure S33. Assessment of DNA binding affinities of Pt-PhN-NEt_2 by fluorescence competitive quenching of EB-DNA adduct.

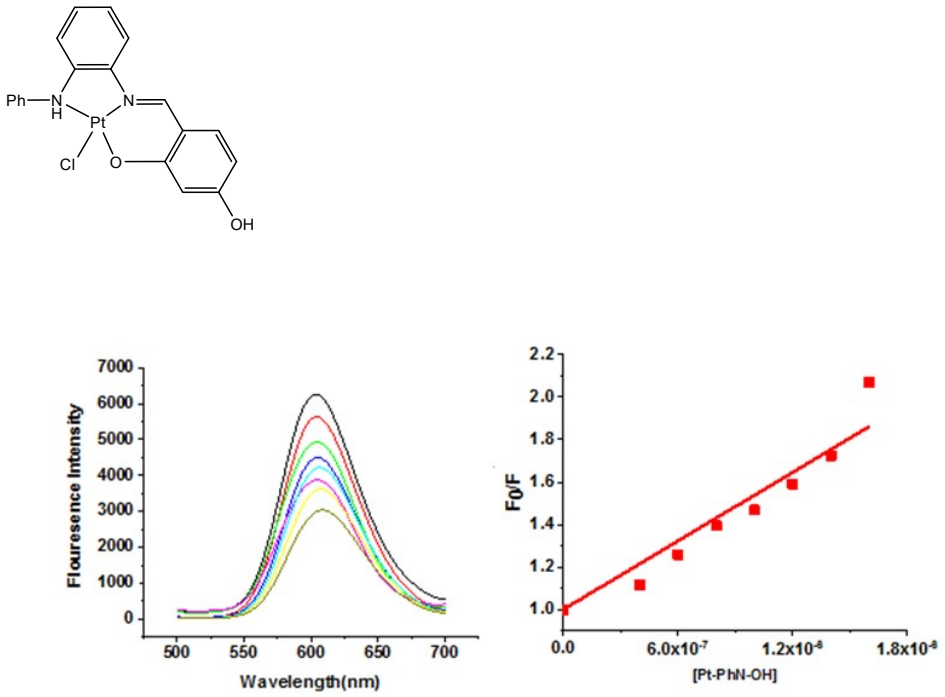

Figure S34. Assessment of DNA binding affinities of Pt-PhN-OH by fluorescence competitive quenching of EB-DNA adduct.

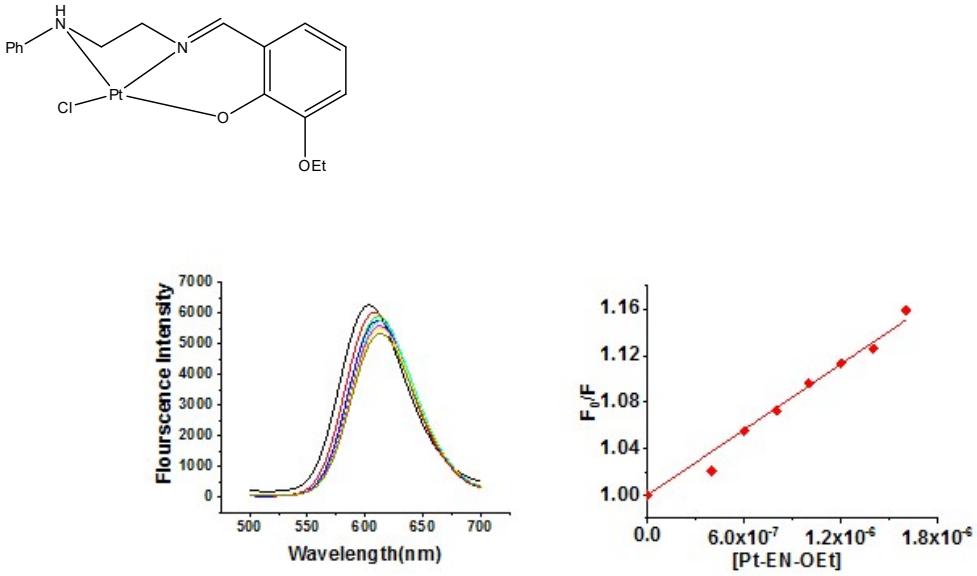

Figure S35. Assessment of DNA binding affinities of Pt-EN-OEt by fluorescence competitive quenching of EB-DNA adduct.

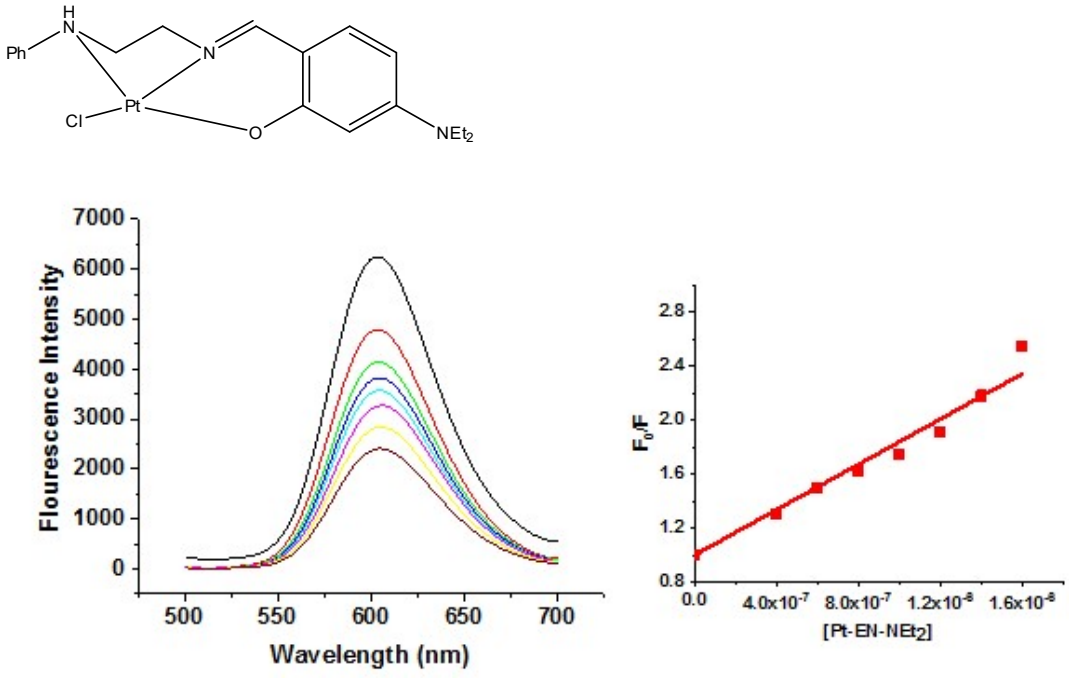

Figure S36. Assessment of DNA binding affinities of Pt-EN-NEt_2 by fluorescence competitive quenching of EB-DNA adduct.

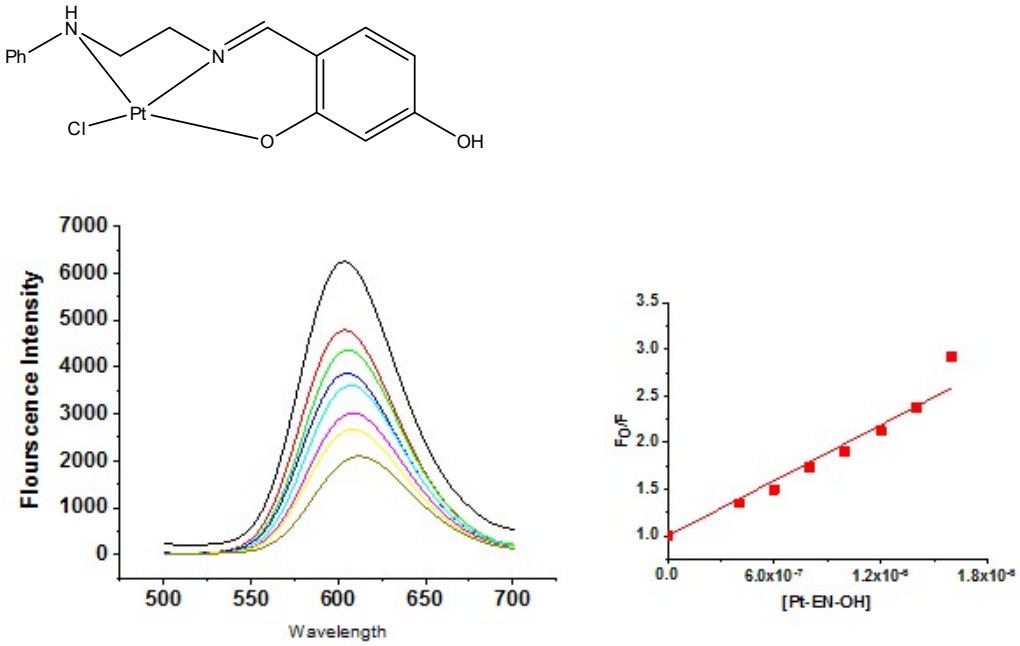

Figure S37. Assessment of DNA binding affinities of Pt-EN-OH by fluorescence competitive quenching of EB-DNA adduct.

Binding Mode by Changes in Relative Viscosity of DNA

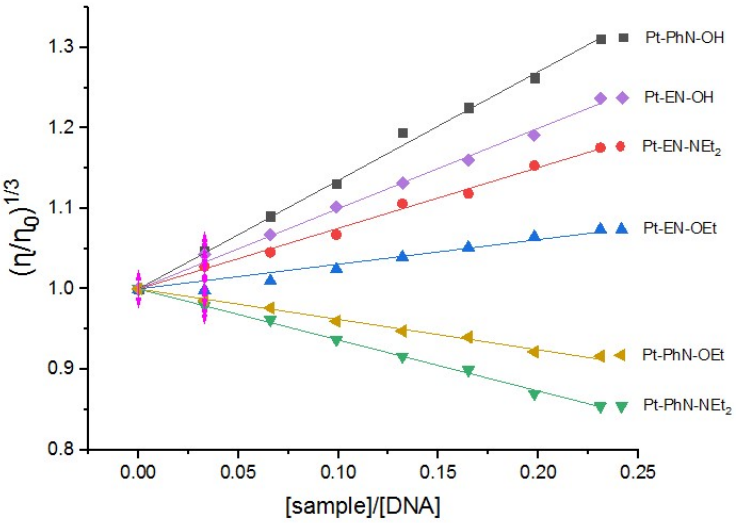

Figure S38. Changes in relative viscosity of ct-DNA upon treatment with platinum(II) complexes.

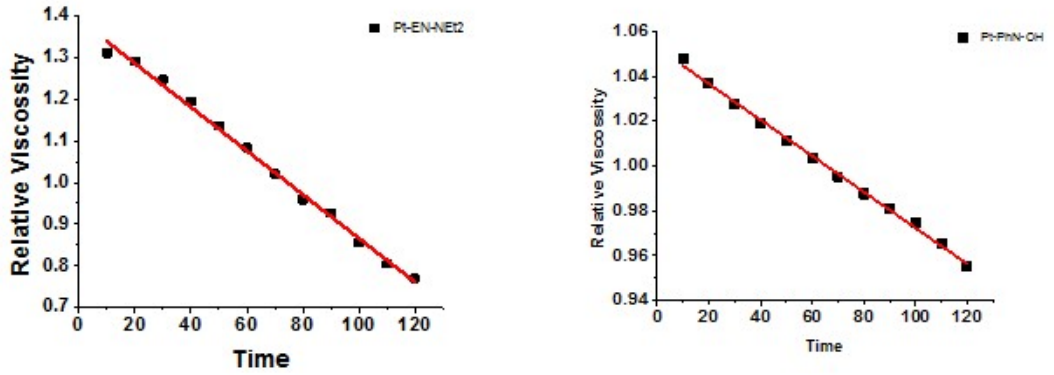

Figure S39. Change in relative viscosity of ct-DNA upon addition of 10 μM Pt-EN-NEt$_2$ and Pt-PhN-OH over 120 min.

Computational Studies

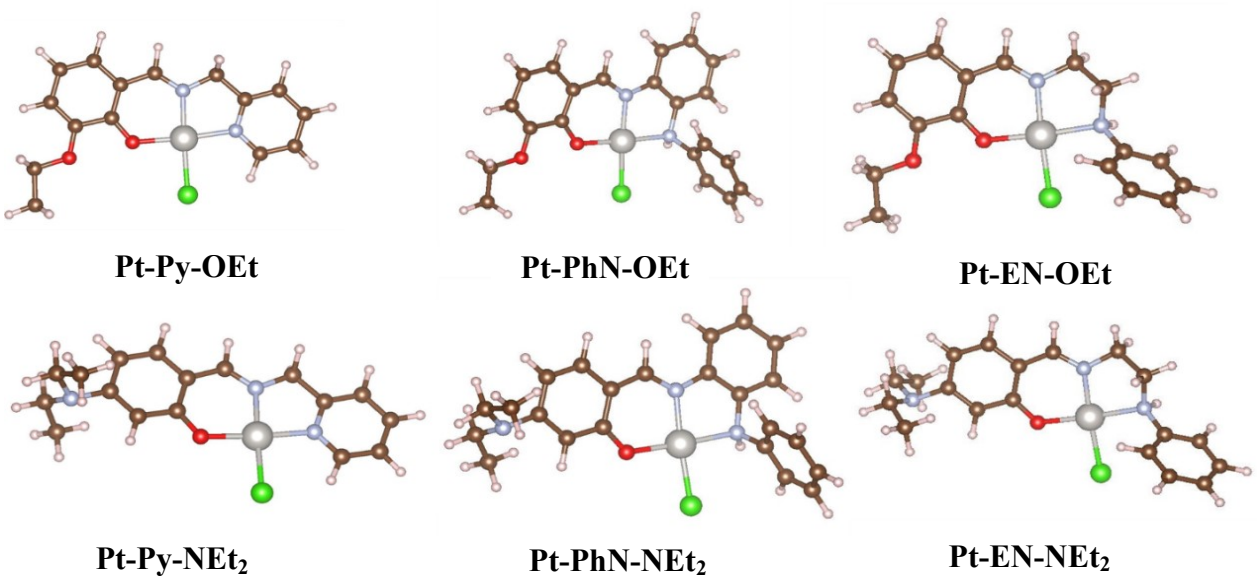

Figure S40. Optimized structures of the different complexes.

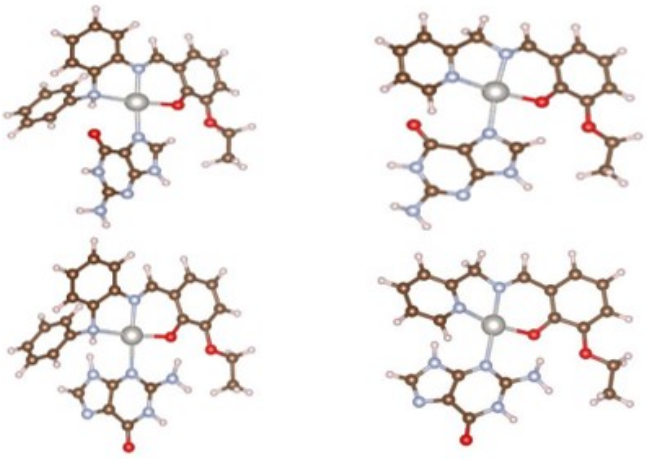

Pt-adduct		Energy (a.u.)	Bonding around the Pt				Hydrogen bonding		ΔE (kcal/mol)
			Pt-N_a	Pt-N_b	Pt-O	Pt-N_G	O-NH_2(G)	H--O_G	
Pt-Py-OEt	N_3-guanine	-1502.578	2.07	2.02	2.03	2.16	2.26		-7.4
	N_7-guanine	-1502.590	2.13	2.04	2.14	2.15		2.80	
Pt-Py-NEt_2	N_3-guanine	-1561.341	2.06	2.00	2.03	2.13	2.45		-6.1
	N_7-guanine	-1561.350	2.11	2.02	2.13	2.14		2.87	
Pt-PhN-OEt	N_3-guanine	-1733.656	2.13	2.01	2.02	2.10	2.25		-4.3
	N_7-guanine	-1733.650	2.16	2.01	2.02	2.15		3.23	
Pt-PhN-NEt_2	N_3-guanine	-1792.417	2.12	2.00	2.02	2.10	2.34		-3.2
	N_7-guanine	-1792.411	2.15	2.01	2.03	2.15		3.31	

N_a the nitrogen of the pyridyl or phenylamine
N_b the nitrogen of the Schiff base

Figure S41. Selected optimized structures for guanine adducts with structural parameters and energies as obtained by theoretical calculations.

Protein Binding Studies

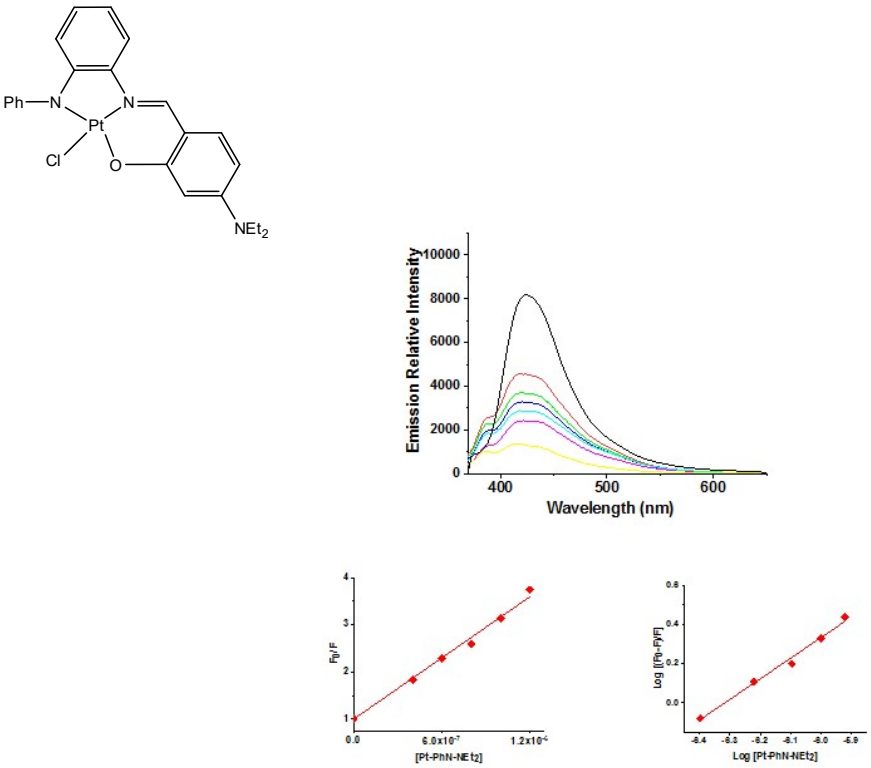

Figure S42. Assessment of Protein binding affinities of Pt-PhN-NEt_2 by fluorescence quenching.

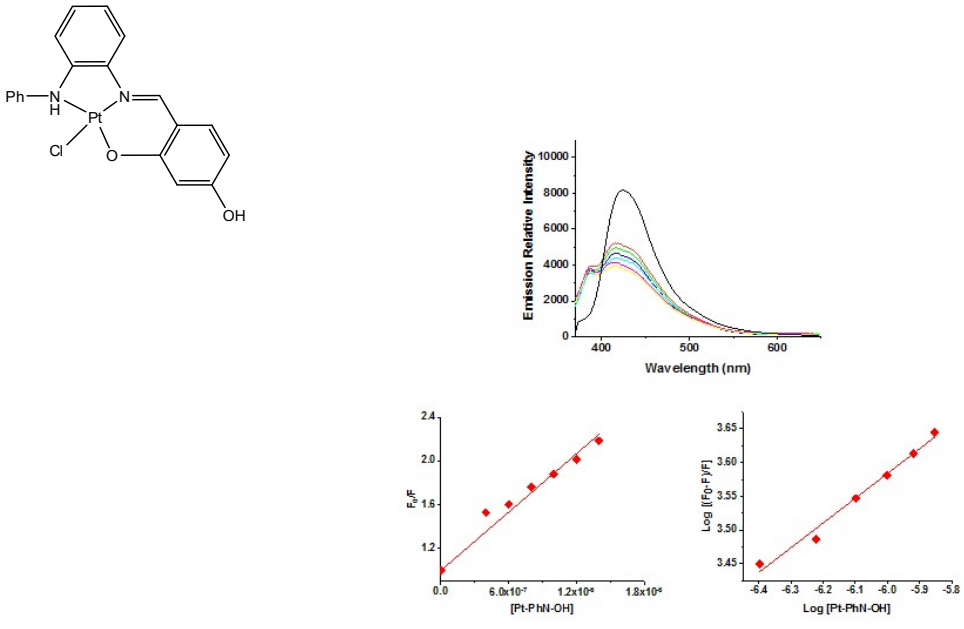

Figure S43. Assessment of Protein binding affinities of Pt-PhN-OH by fluorescence quenching.

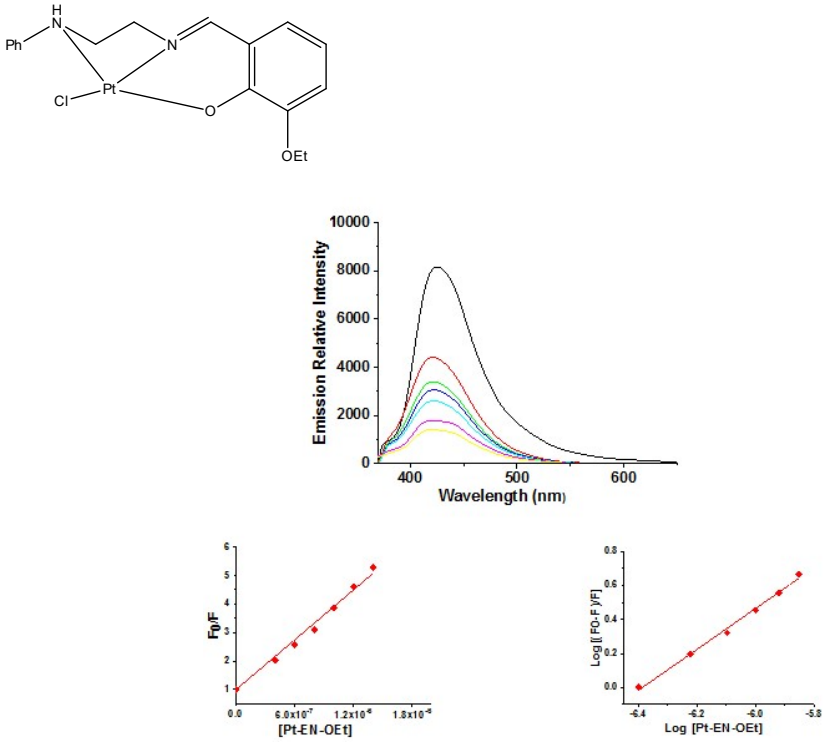

Figure S44. Assessment of Protein binding affinities of Pt-EN-OEt by fluorescence quenching.

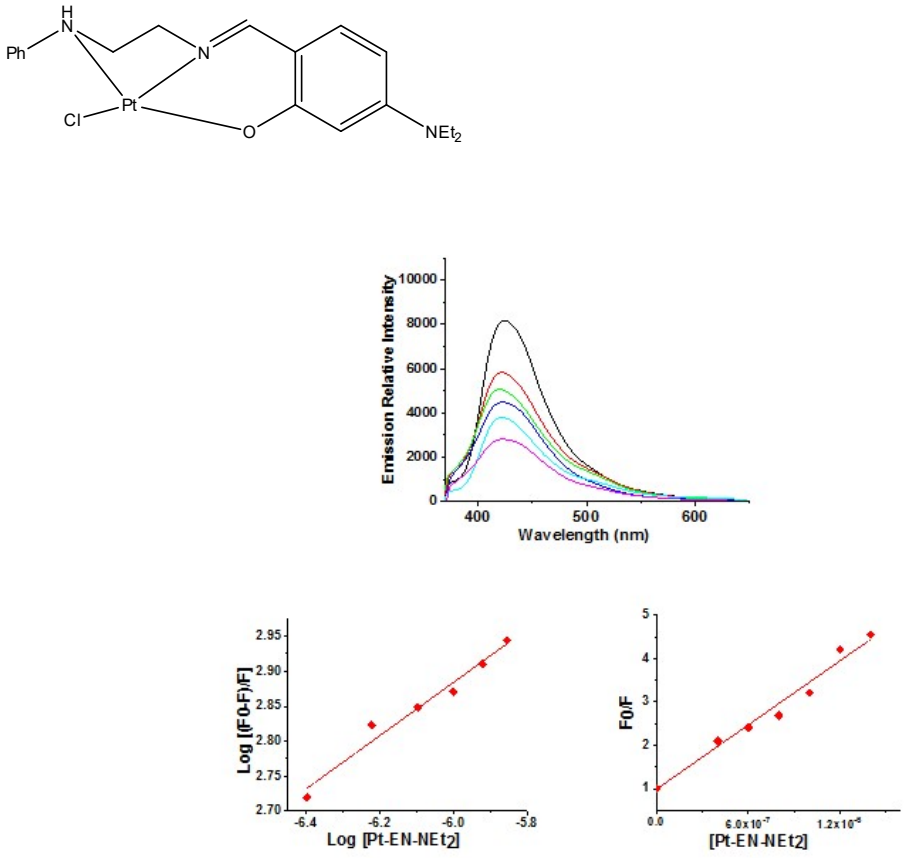

Figure S45. Assessment of Protein binding affinities of Pt-EN-NEt_2 by fluorescence quenching.

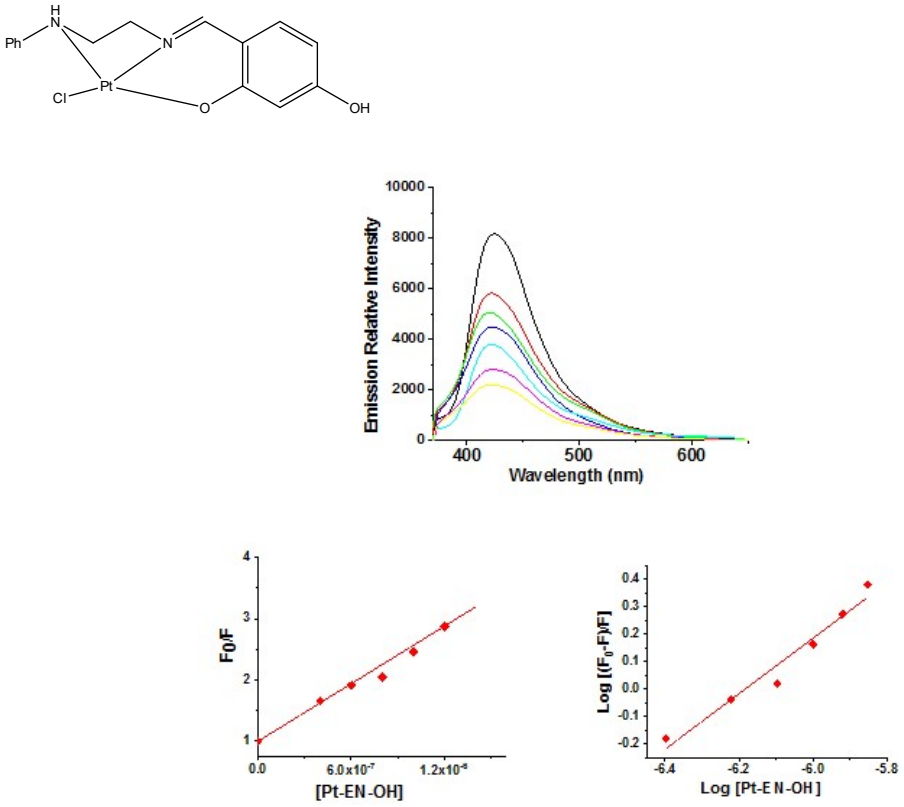

Figure S46. Assessment of Protein binding affinities of Pt-EN-OH by fluorescence quenching.

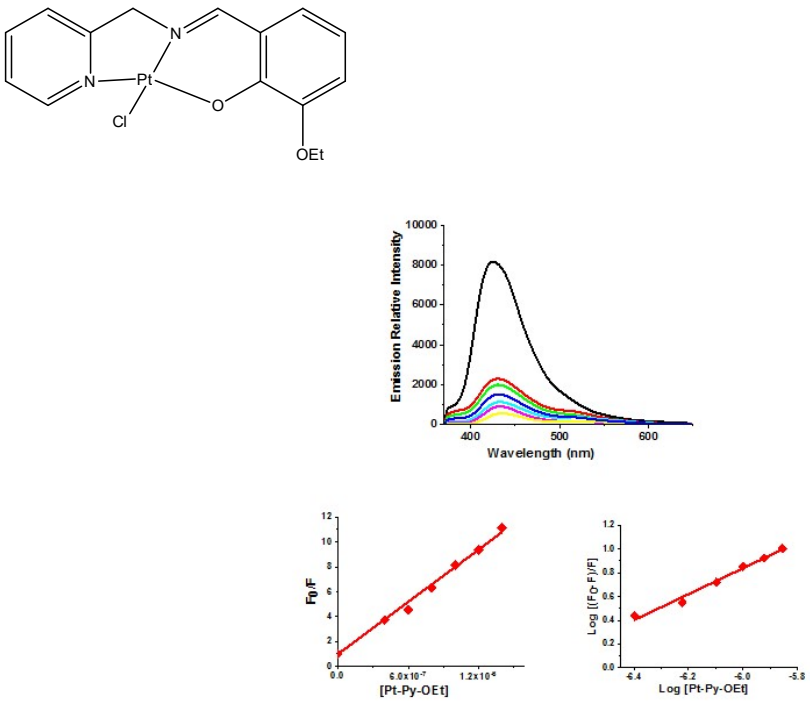

Figure S47. Assessment of Protein binding affinities of Pt-Py-OEt by fluorescence quenching.

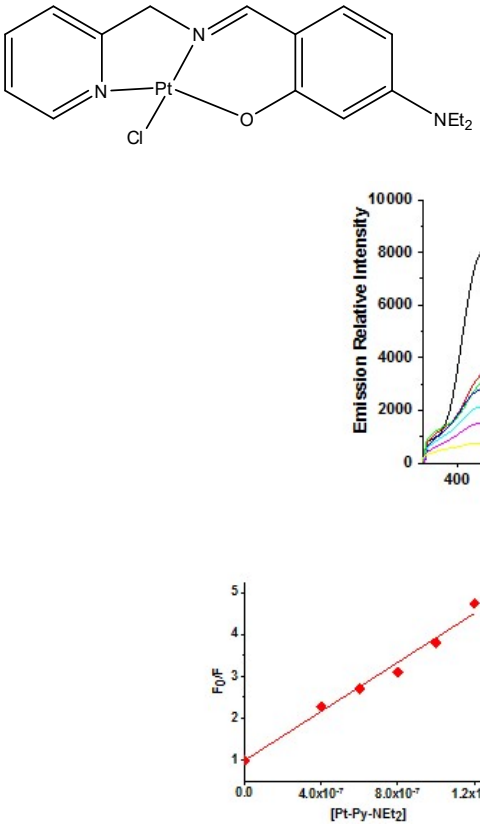

Figure S48. Assessment of Protein binding affinities of Pt-Py-NEt_2 by fluorescence quenching.

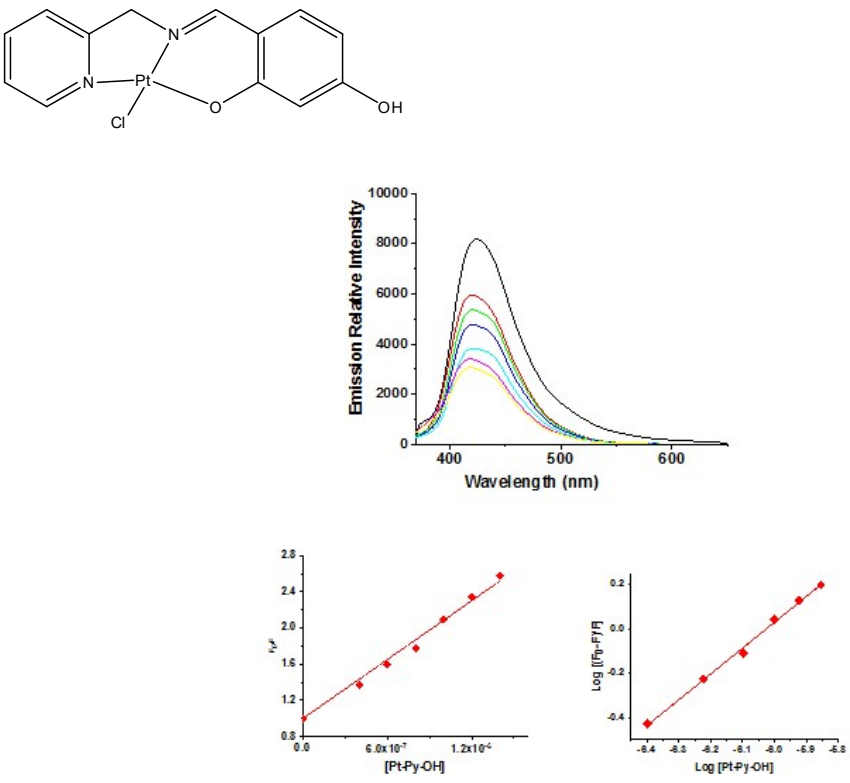

Figure S49. Assessment of Protein binding affinities of Pt-EN-OEt by fluorescence quenching.

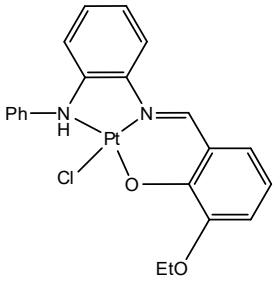

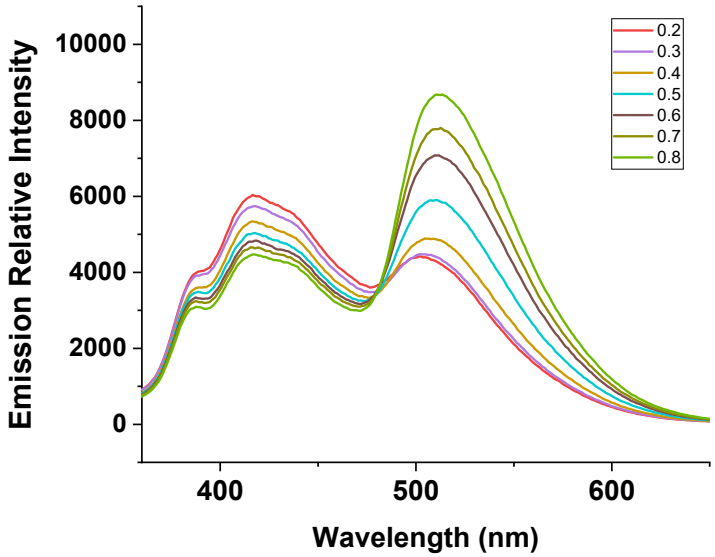

Figure S50. Assessment of Protein binding affinities of Pt-PhN-OEt by fluorescence quenching.

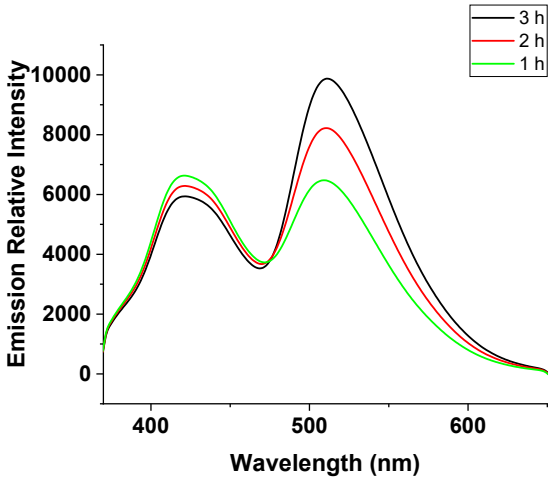

Figure S51. Assessment of Protein binding affinities of Pt-PhN-OEt y by fluorescence quenching with different time.

Preliminary *in vitro* Antiproliferative Activity

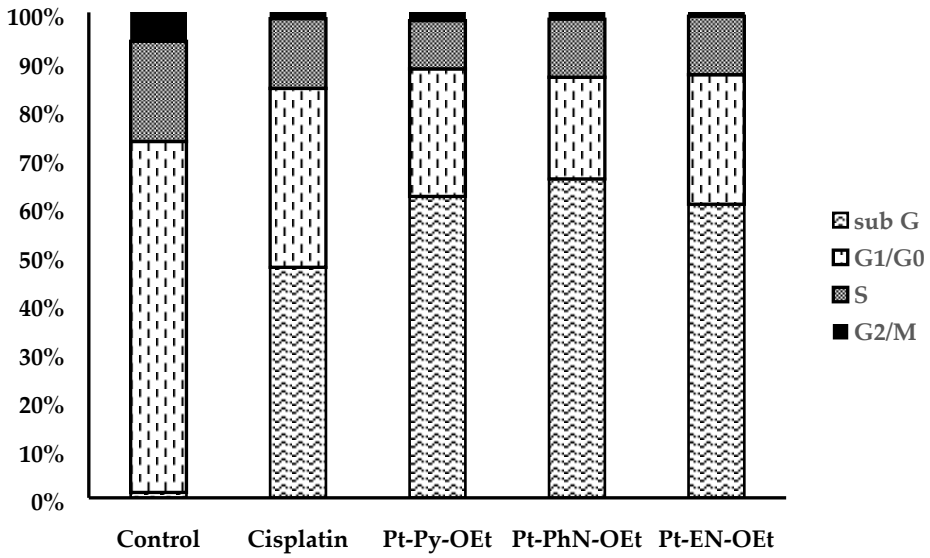

Figure S52. Cell cycle assay of HepG-II upon treatment with different compounds.